Gone with the Wind

Astrophysical deductions from Amber differential measurements on massive hot stars (MWC297, α Arae, η Carinae, γ^2 Velorun, …)

EuroSummer School

Observation and data reduction with the Very Large Telescope Interferometer

Goutelas, France
June 4-16, 2006

Romain G. Petrov
Université de Nice Sophia – Antipolis
LUAN: UMR 6525 UNSA/CNRS

7 June 2006

Introduction

- First AMBER observations in GTO and in SDT (12/04 and 2/05)
- Poor absolute visibilities
- Good color differential measures
- Noisy but « calibration free » closure phases
- Well studied stars with emission lines: massive hot stars with wind
- UT time: poor u-v coverage
- How to use spatial information with poor u-v coverage bu good spectral features ?

Plan

- Amber specifications and measures
- Herbig star MWC 297 and the use of differential visibility on a single baseline
- The Be star α Arae: full Amber package ($V(\lambda),\Phi(\lambda),\Psi_{123}(\lambda)=0$) and differential interferometry like in the manual
- The LBV η Carinae: all measures and closure phase non zero in the line
- The γ^2 Vel WR in a binary system and the specific input of closure phase
- Steps toward extra solar planets spectroscopy
- Conclusion

AMBER, what is it?

Combines 2 or **3 beams**

Spectrograph:

- Spectral coverage:
  - [1-2.5µm] (J, H, K)
- Spectral resolution:
  - 35, 1500, 12000

Observables:

- Visibilities for 3 baselines
- Colour-differential phases and visibilities for 3 baselines
- Closure phase

► Spectral coverage, spectral resolution and better sensitivity give access to many new astrophysical fields

AMBER Layout for the K band

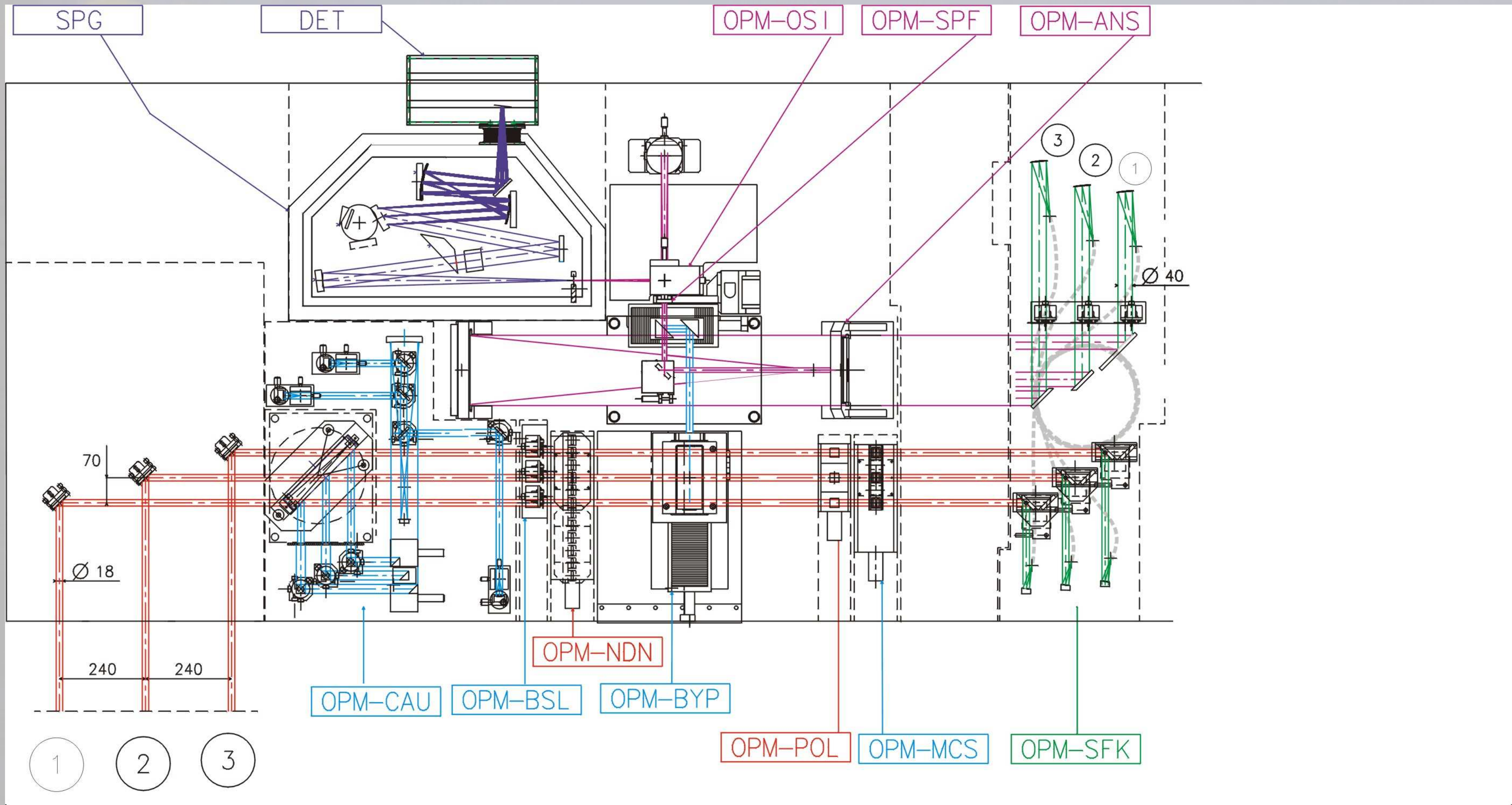

Panoramic view of AMBER for J,H and K

(Grenoble integration and test room)

size: L=4.2 m, W=1.5 m, H=2m; weight~1800 Kg

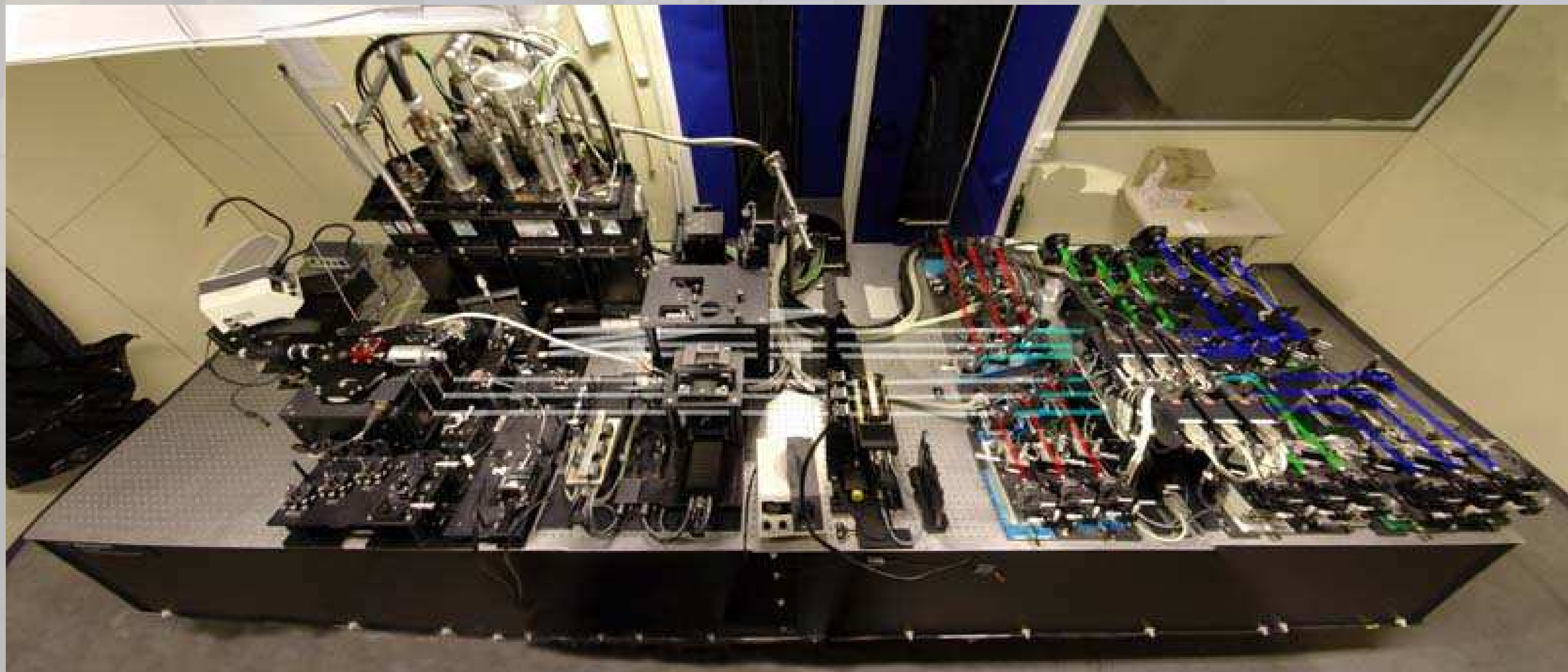

Internal Calibration Fringes (LR_JHK)

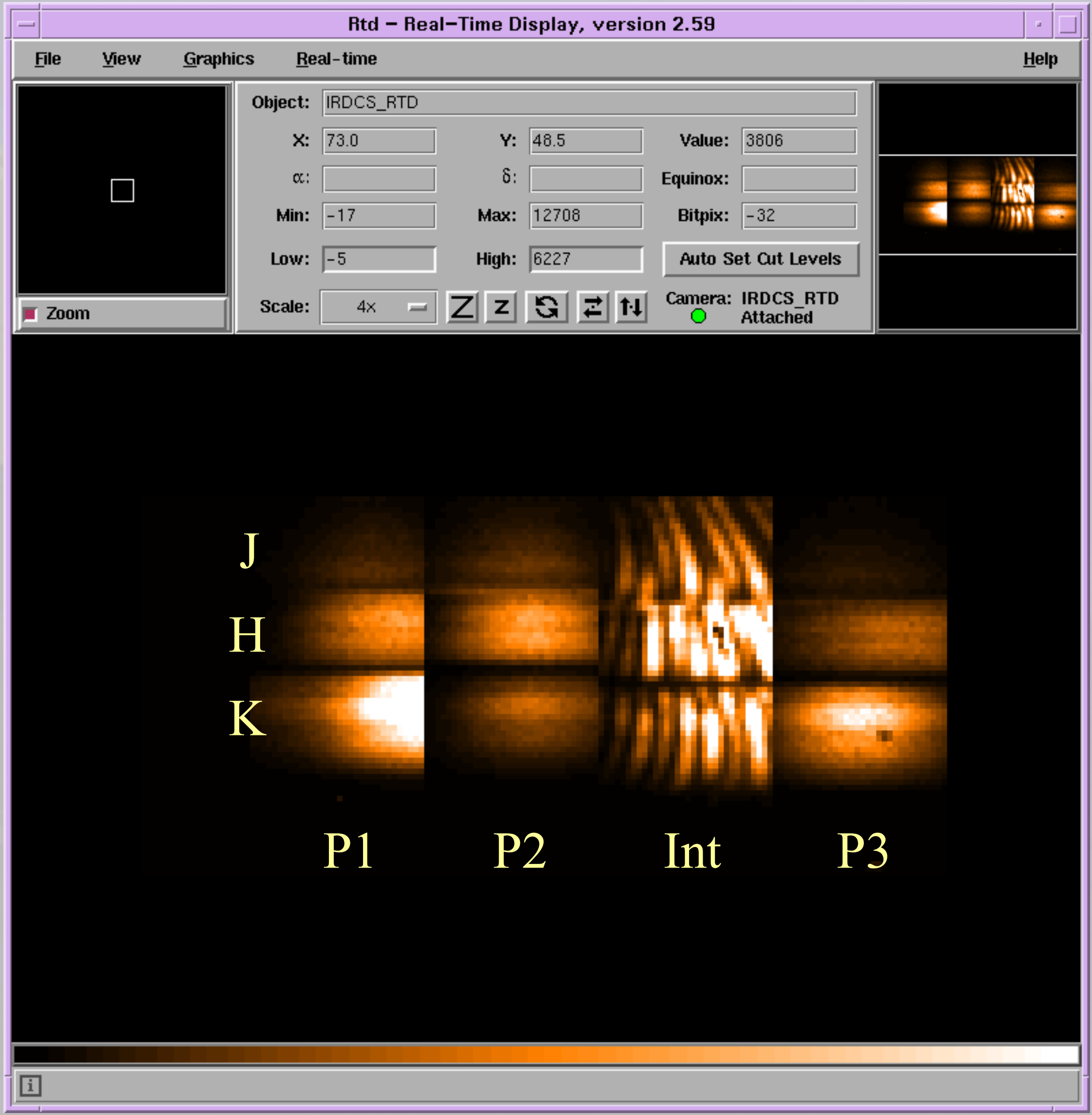

AMBER measures

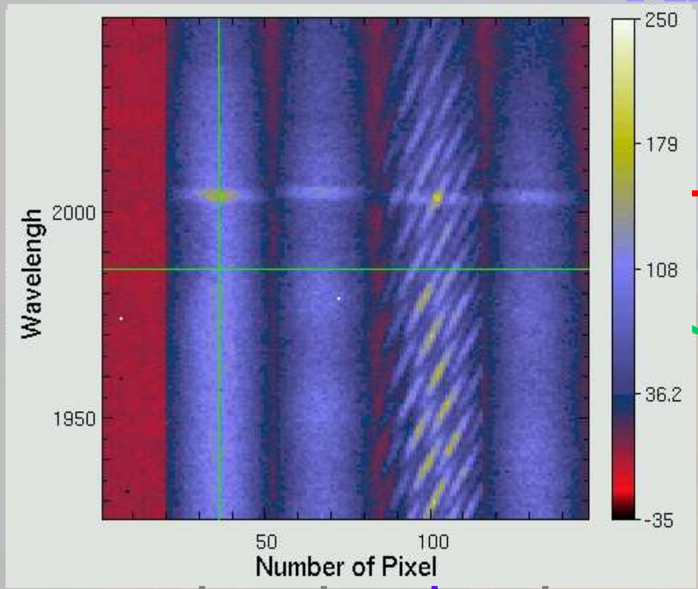

Work channel at λ: $C_i(\lambda)$

Reference channel averaged over Δλ: $C_{i\ ref}=\sum_{\Delta\lambda} C_i(\lambda)$

Photometric beams

Interferometric beam

Complex Visibility per frame: $C_i(\lambda)$
(corrected for the achromatic piston)

- Spectrum $S(\lambda)$
- Visibility = $V_i(\lambda) = <|C_i(\lambda)|^2>_{frames}$
- Differential Visibility: $V_{id}(\lambda) = \mathrm{Re}[<C_i(\lambda)C_{iref}^*>_{frames}]$
- Differential visibility: $\Phi_{id}(\lambda) = \tan^{-1}(<C_i(\lambda)C_{iref}^*>_{frames})$
- Closure phase: $\Psi_{123}(\lambda) = \tan$-1$[<C_1(\lambda)\ C_2(\lambda)\ C_3^*(\lambda)>_{frames}]$
- "Closure" of differential phases: $\Psi_{d123}(\lambda)=\Phi_{1d}(\lambda)+\Phi_{2d}(\lambda)-\Phi_{3d}(\lambda)$

The Herbig Be star MWC297

- Pre Main Sequence Star B1.5V
  - Strong emission lines
  - Strong IR excess
- Mass=10 $M_{\odot}$. Radius=6.12 $R_{\odot}$. Distance=250 pc. T_{eff}=23 700 K
- From interferometric observations: ring like disk with puffed up inner rim
  - Inner rim is closer than dust sublimation radius in HBe stars

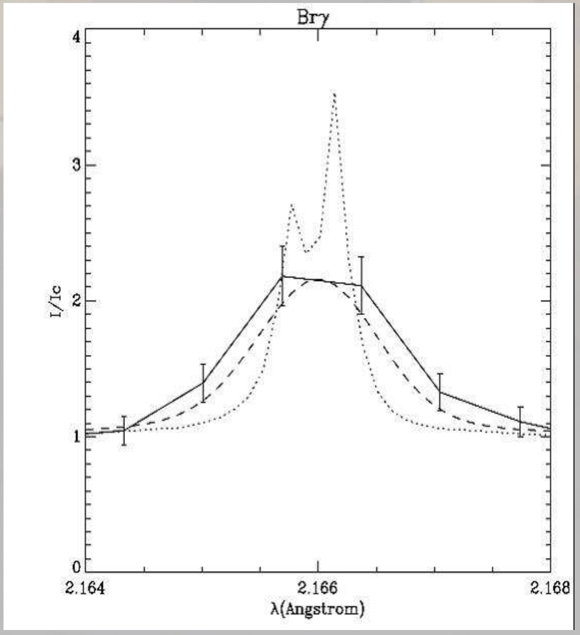

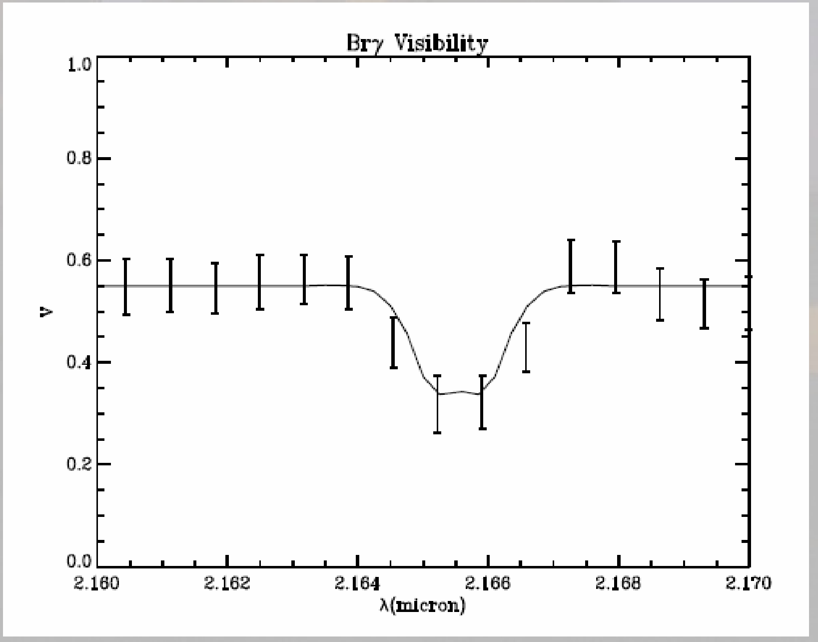

Visibility measurements on MWC 297 parameters of the disk

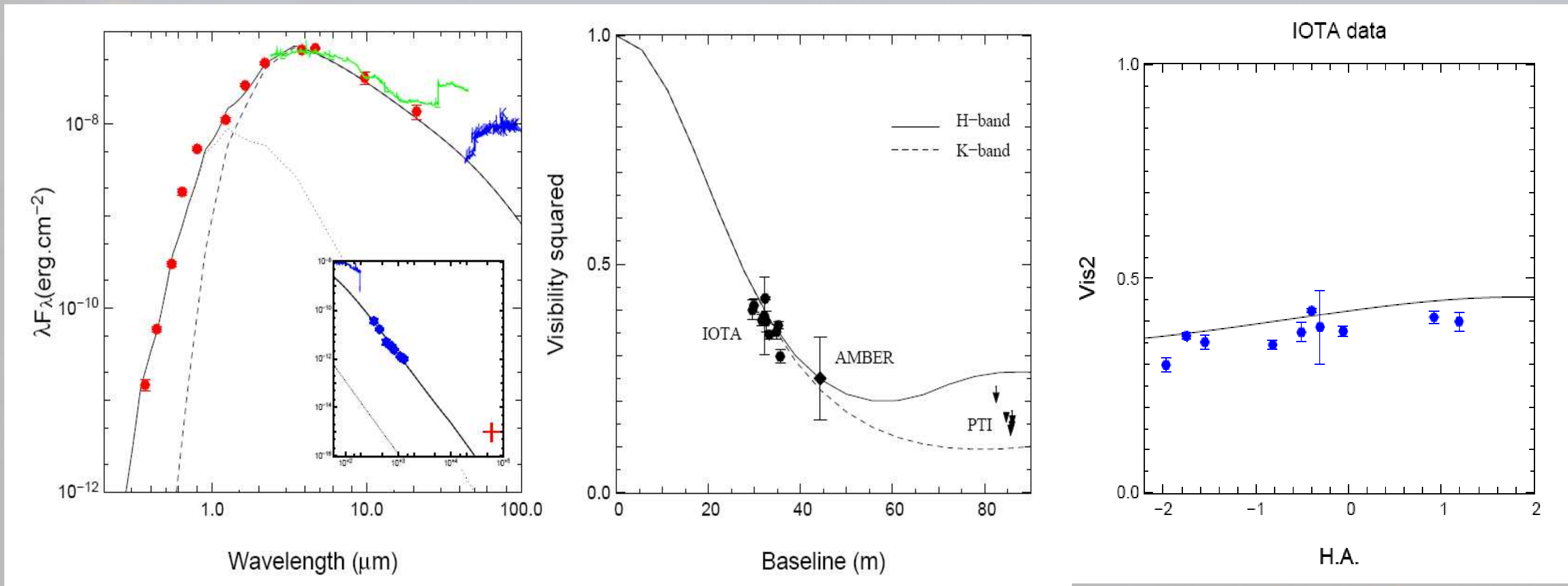

SED → Accretion rate, Inner radius

Radio → Outer radius

Interferometric visibilities → Inclination, Position angle

Accretion rate ($\dot{M}_{acc}$)	$0 - 1 \times 10^{-5}\ M_\odot\ yr^{-1}$
Inner radius (R_{in})	0.5 ± 0.1 AU
Outer radius (R_{out})	55 ± 5 AU
Inclination (i)	$15 \pm 5°$
Position angle (θ)	$56 \pm 7°$

MWC297: the emission line

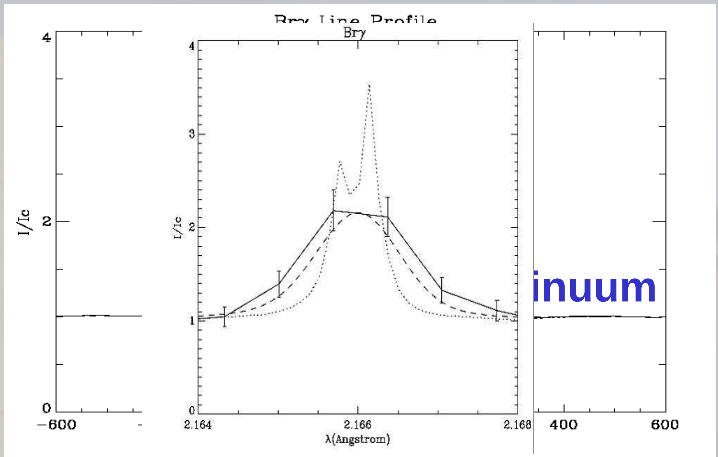

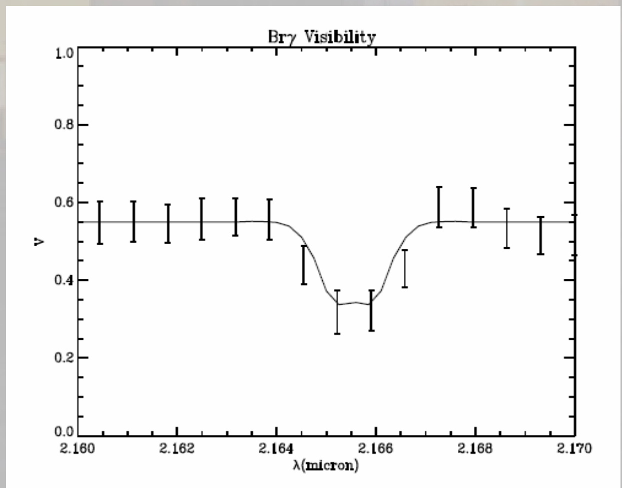

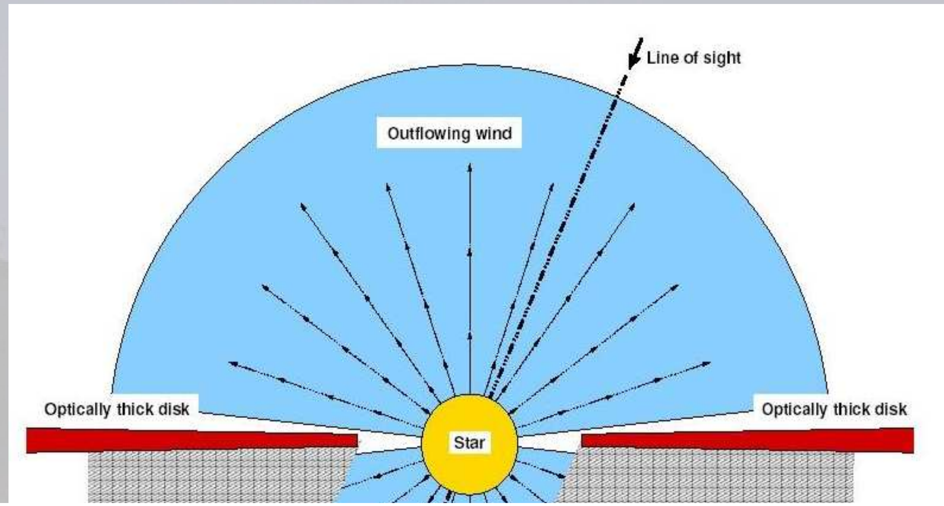

Photospheric density	$1 \pm 0.5 \times 10^{12}$ cm^{-3}
Equatorial rotational velocity	400 ± 50 km s^{-1}
Polar terminal velocity	600 ± 50 km s^{-1}
Terminal velocity above disk	70 ± 20 km s^{-1}
Polar mass flux	$3.2 \pm 0.2 \times 10^{-9}$ $M_\odot$ yr^{-1}
C_1	0.25 ± 0.05
m_1	30 ± 10
m_2	10 ± 2
Inclination angle (i)	$25 \pm 5°$

Malbet et al. (2005, A&A astro-ph/0510350)

MWC 297

- Succesfull disk + wind modeling
- One differential visibility measurement allows to choose between options for a well known object when combined to all other data
- Inclination discrepancy: if the star had a i=20°, its rotation velocity would be > 1000 Km/s.
- Disk and wind warped by unknown companion.
- Next observations: 3 baselines of course but privilege spectral resolution other u-v coverage.

The Be star α Arae

The classical Be star: B3Ve, T_{eff}=18000K, M_*= 9.6$M_\odot$, R_*= 4.8$R_\odot$, L_*= 5.8 10^3 $L_\odot$, i=45°, v_e sin$i$=300 km/s, $v_{e\infty}$=179 km/s, $v_{p\infty}$=2000 km/s

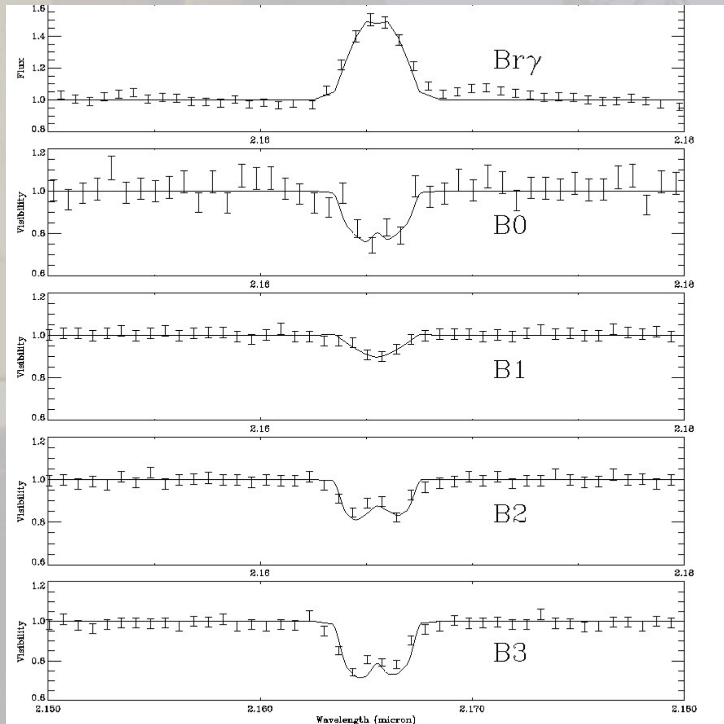

Line profile and Differential visibility

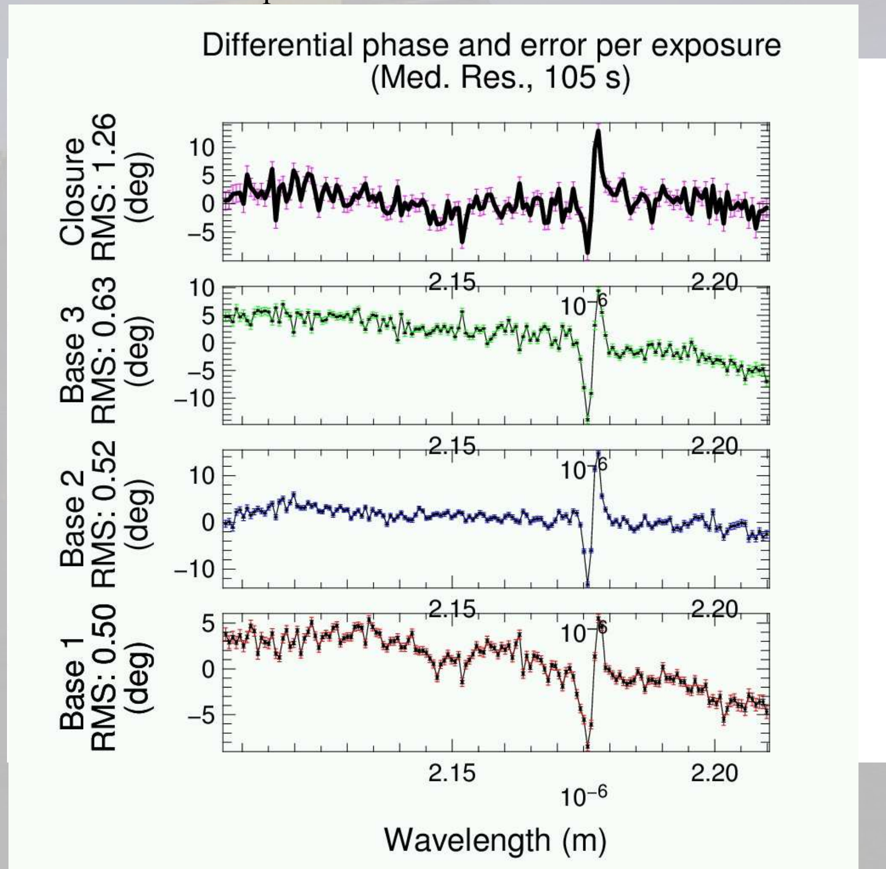

Differential phase

Visibility measures on α Arae

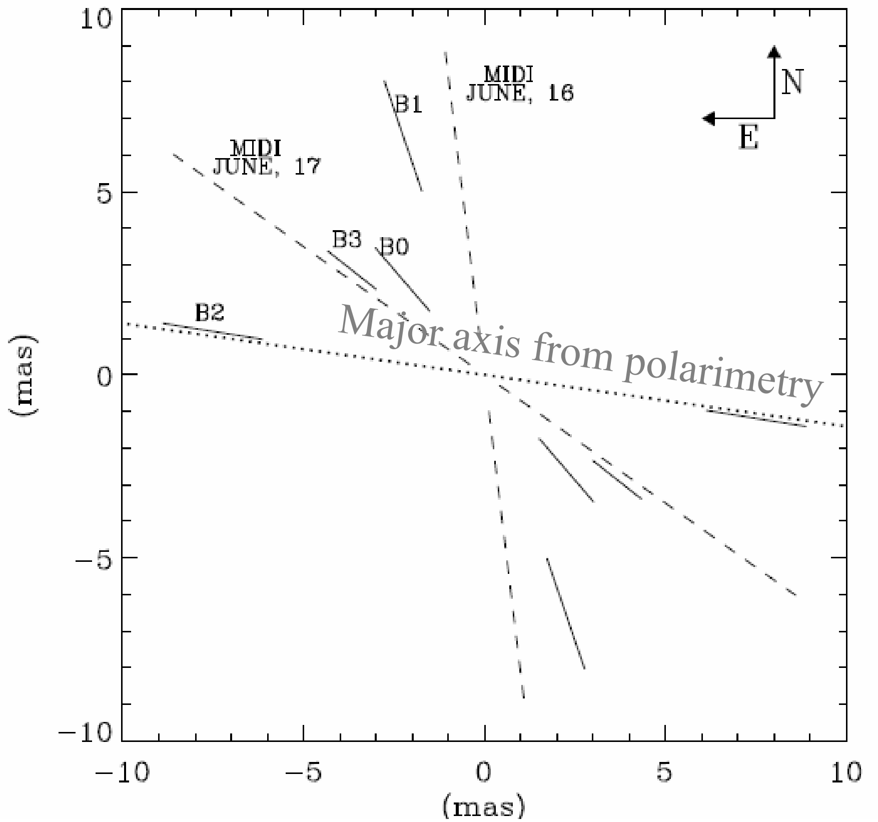

Continuum visibilities converted in disk+star equivalent diameter.

Toy models to fit the continuum visibilities

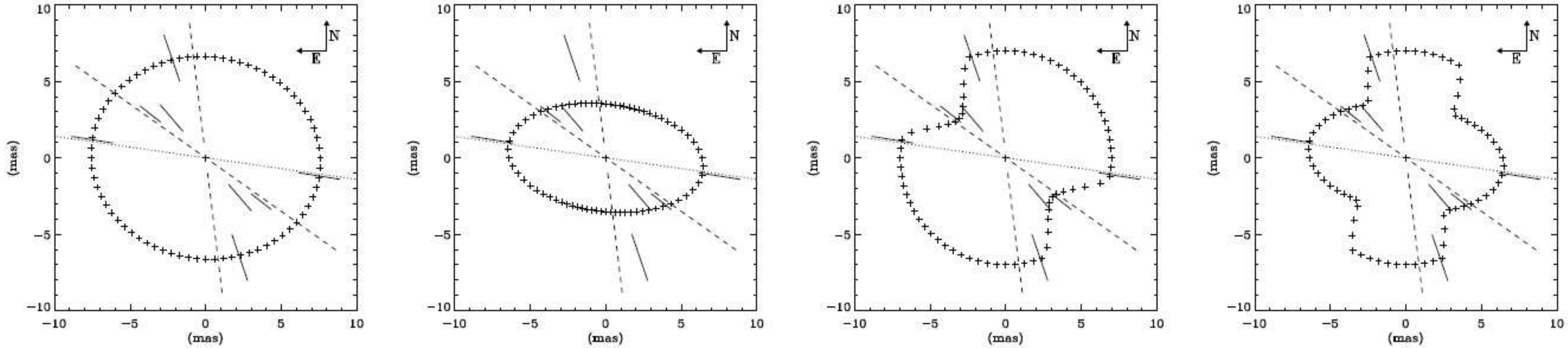

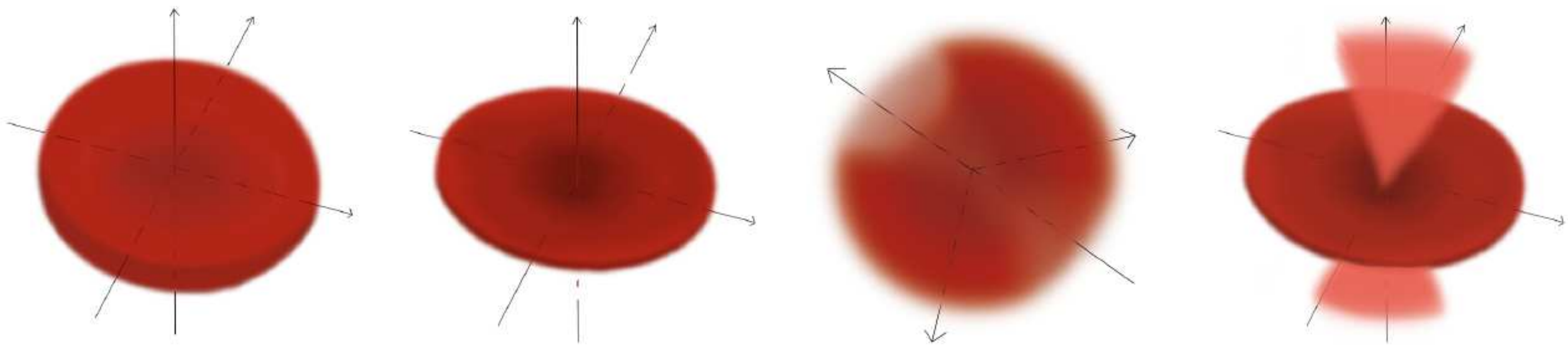

Disc :
Diameter = 7.6 mas
Opening angle = 25°
Inclination anlge = 45°

Disc :
Diameter = 6.5 mas
Opening angle = 2°
Inclination anlge = 57°

Envelope :
Diameter = 7 mas
Opening angle = 120°
Inclination anlge = 45°
Minor axis in the orientation of base 3

Disc :
Diameter = 6.5 mas
Opening angle = 2°
Inclination anlge = 57°
Polar jets :
Diameter = 7 mas
Opening angle=50°

The SIMECA code

- Computes line profiles, SED, intensity maps yielding interferometric observables
- Axi symmetric enveloppe. No meridional circulation.
- Inner equatorial region dominated by rotation and quasi Keplerian
- Ionization-excitation equations solved in a 3D grid of 410*90*71 elements
- Iterative computation of non LTE conditions
- Mass flux and expansion velocity vary as a function of latitude

SIMECA parameters and best fit for α Ara

Latitudinal variation of mass flux:

$$\Phi(\theta) = \Phi_{pole}[1 + (C1 - 1)\sin^{m1}(\theta)].$$

$$C1 = \frac{\Phi_{eq}}{\Phi_{pole}}.$$

Expansion velocity field:

$$v_r(r,\theta) = V_o(\theta) + [V_\infty(\theta) - V_o(\theta)](1 - \frac{R}{r})^\gamma,$$

$$V_o(\theta) = \frac{\Phi(\theta)}{\rho_0} = \frac{\Phi_{pole}[1 + (C1 - 1)\sin^{m1}(\theta)]}{\rho_0}.$$

Terminal Velocity:

$$V_\infty(\theta) = V_\infty(pole) + [V_\infty(eq) - V_\infty(pole)]\sin^{m2}(\theta).$$

parameter/result	value
$v \sin i$	375 km s^{-1}
Inclination angle i	55°
Photospheric density (ρ_{phot})	1.0 10^{-11}g cm^{-3}
Equatorial rotation velocity	470 km s^{-1}
Equatorial terminal velocity	1 km s^{-1}
Polar terminal velocity	1000 km s^{-1}
Polar mass flux	7 $10^{-9} M_\odot$ $year^{-1}$ sr^{-1}
m1	0.5
m2	100.0
C1	0.03
Mass of the disk	4.1 $10^{-10} M_\odot$
Mass loss	1.3 $10^{-8} M_\odot$ $year^{-1}$

A gas envelope in Keplerian rotation around the Be star α Ara

(a question since 1866…)

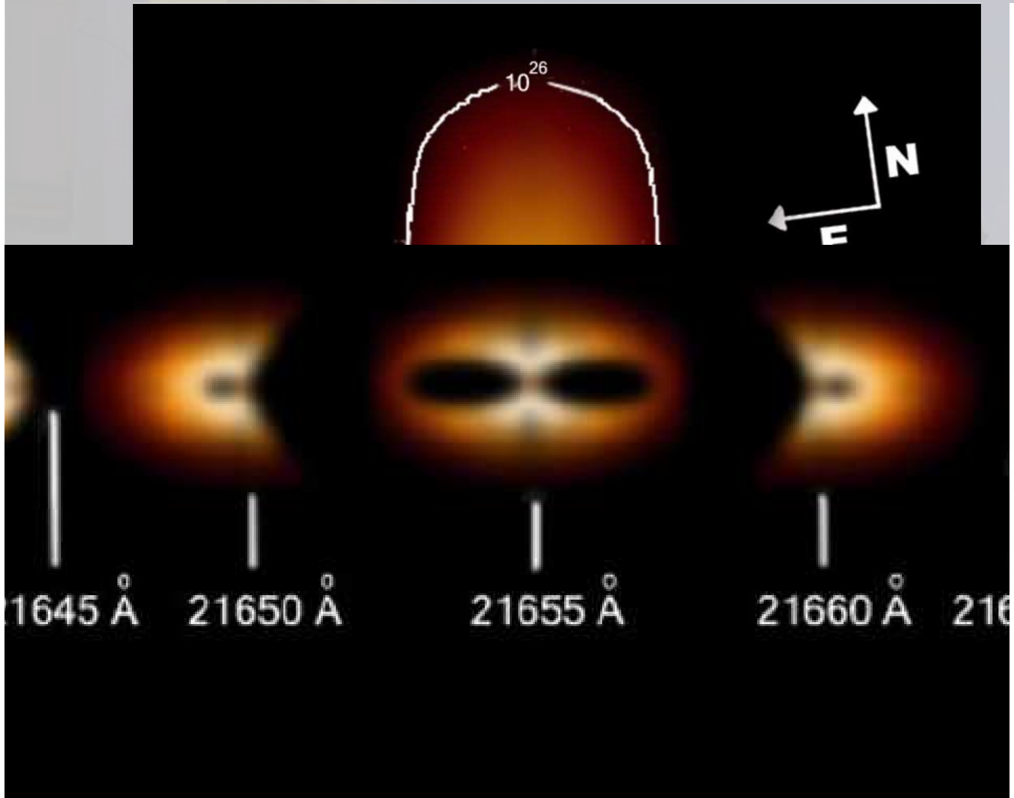

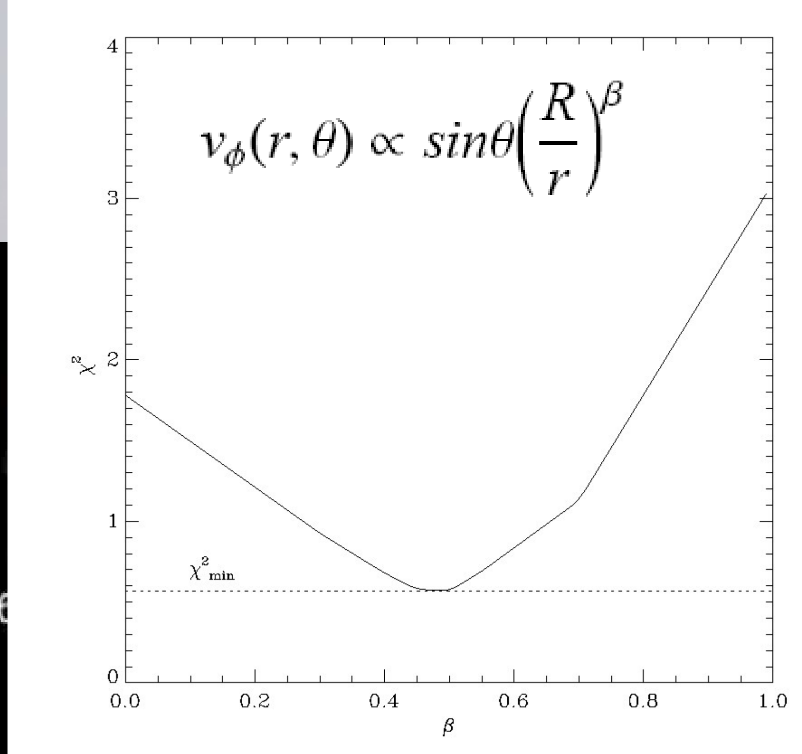

Brightness map computed by the SIMECA code (cont @ 2µm)

0 = constant rotation
0.5 = Keplerian rotation
1 = constant angular momentum

Meilland, A. et al. 2006, A&A, in press

Fit of α Arae measurements

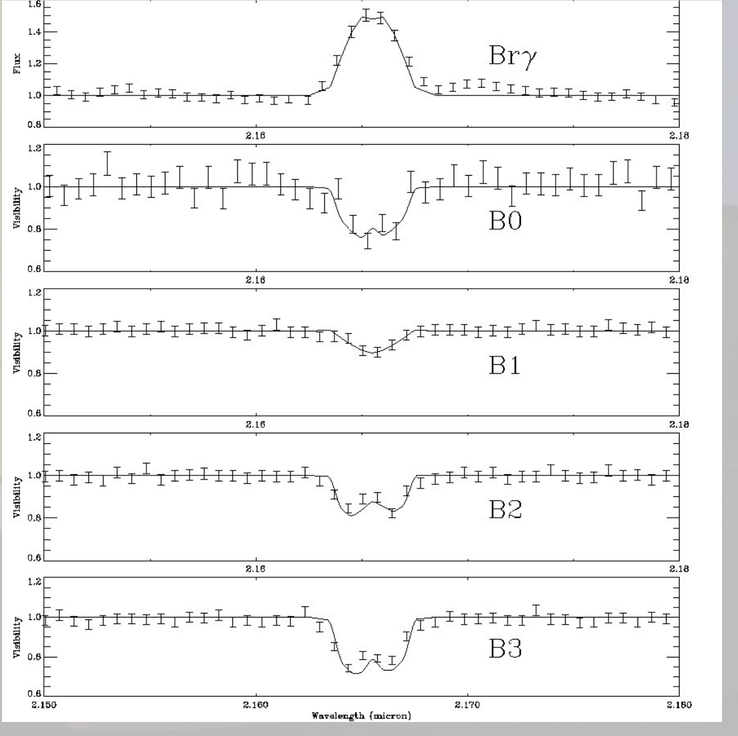

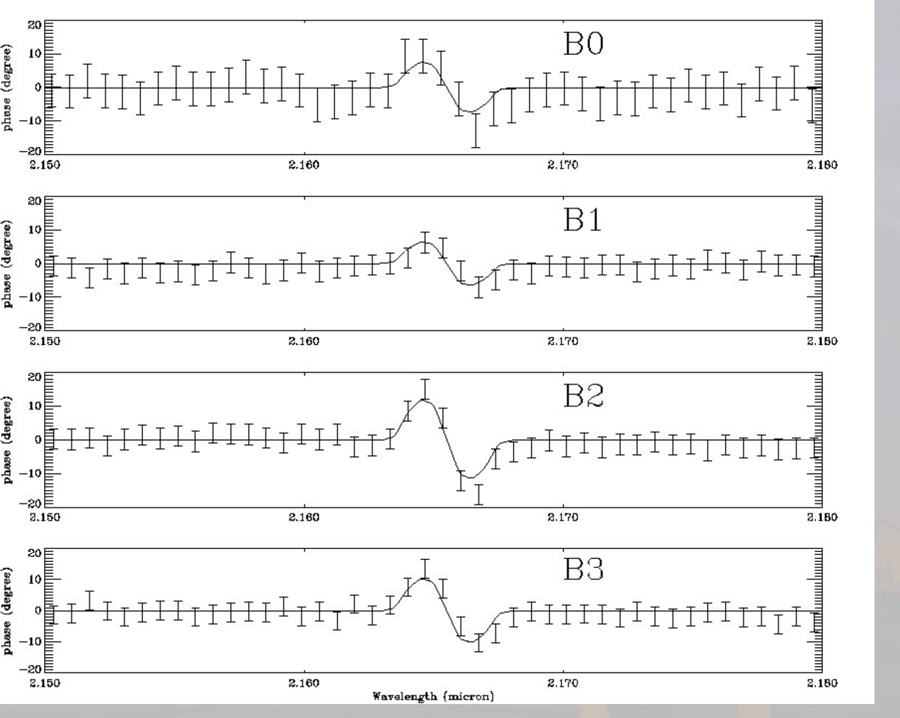

Line profile and Differential visibility

Differential phase

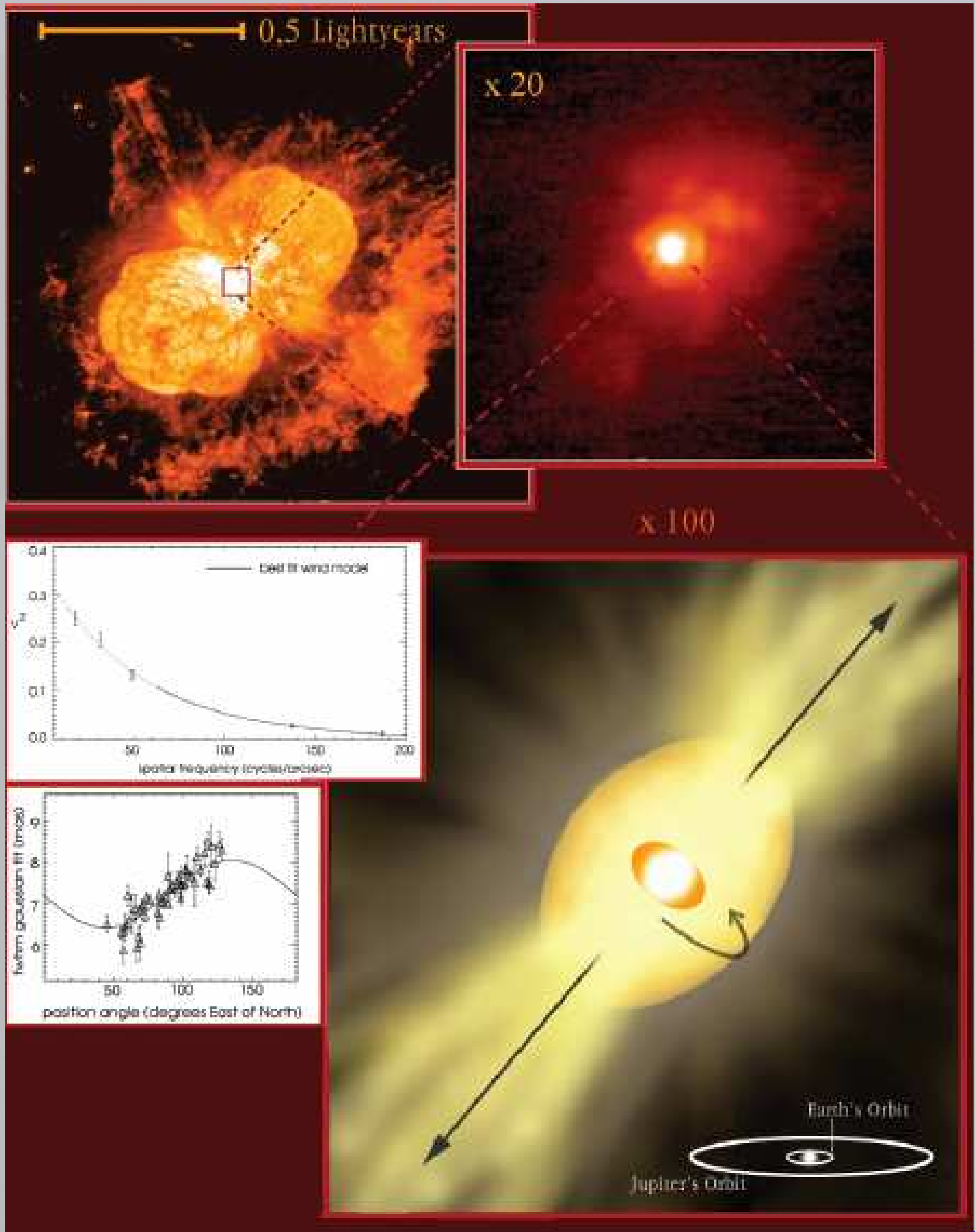

η Carinae

- L = 5 x 10^6 Lsun
- dM/dt = 5 x 10^{-3} Msun/yr
- 500km/s wind
- 60% of flux in the core of the AO image
- Contamination in single mode fibers evaluated from NACO images
- VINCI data resolves the central core: 5 mas (10AU)
- elongated along the flow axis

The luminous blue variable : η Carinae

Massive stars

Visibility

Differential phase (degree)

Closure phase (degree)

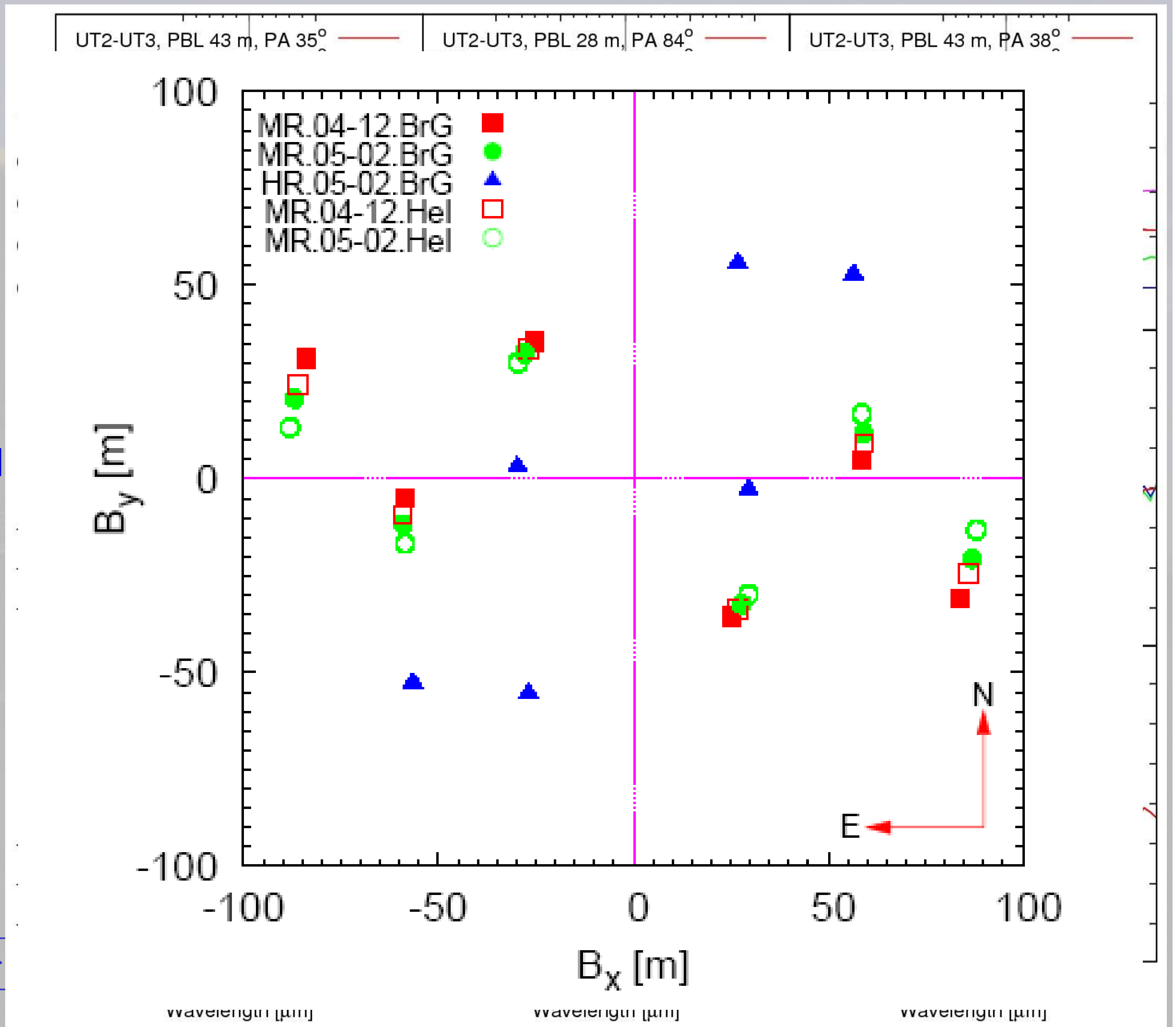

Wind center to limb profiles

Comparison of the measured visibilities with the predictions of the Hillier et al. 2001 model (red lines)

2.174 µm continuum:

Green squares: AMBER
Blue triangles: VINCI
(van Boekel et al. 2003)
Red lines: Hillier model

2.1661 µm
(Br γ emission line):

2.058 µm
(He I emission line):

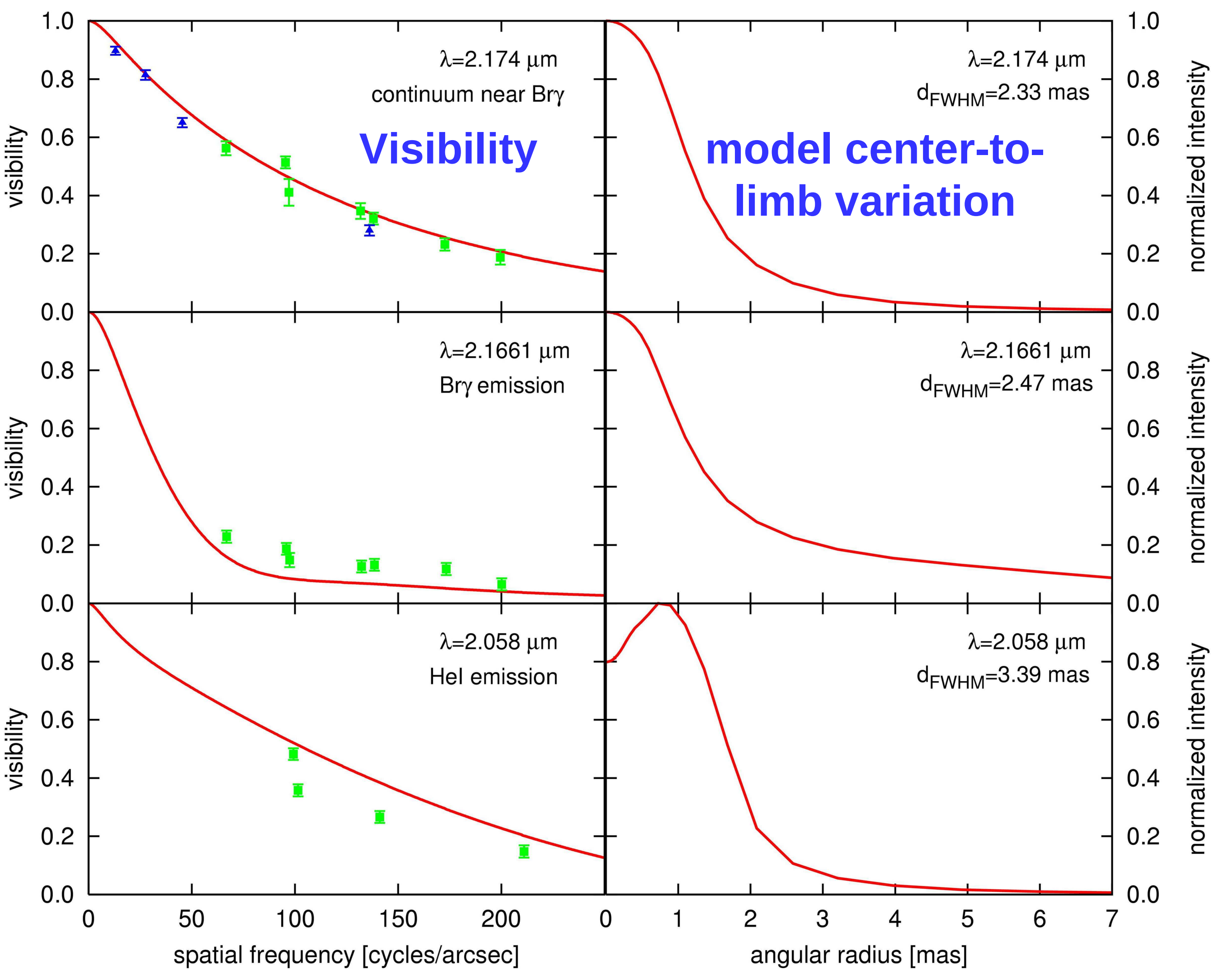

Wind elongation

- Equivalent width from Hillier model as a function of (α,δ)
- Elongation with **PA=128°±15°** (all data, 2D fit)
- Axis ratio **1.21 ± 0.08**
- Elongation in the direction of nebula axis
- Enhanced polar flux
- Compatible with VINCI data (Van Boeckel et al., 2003)

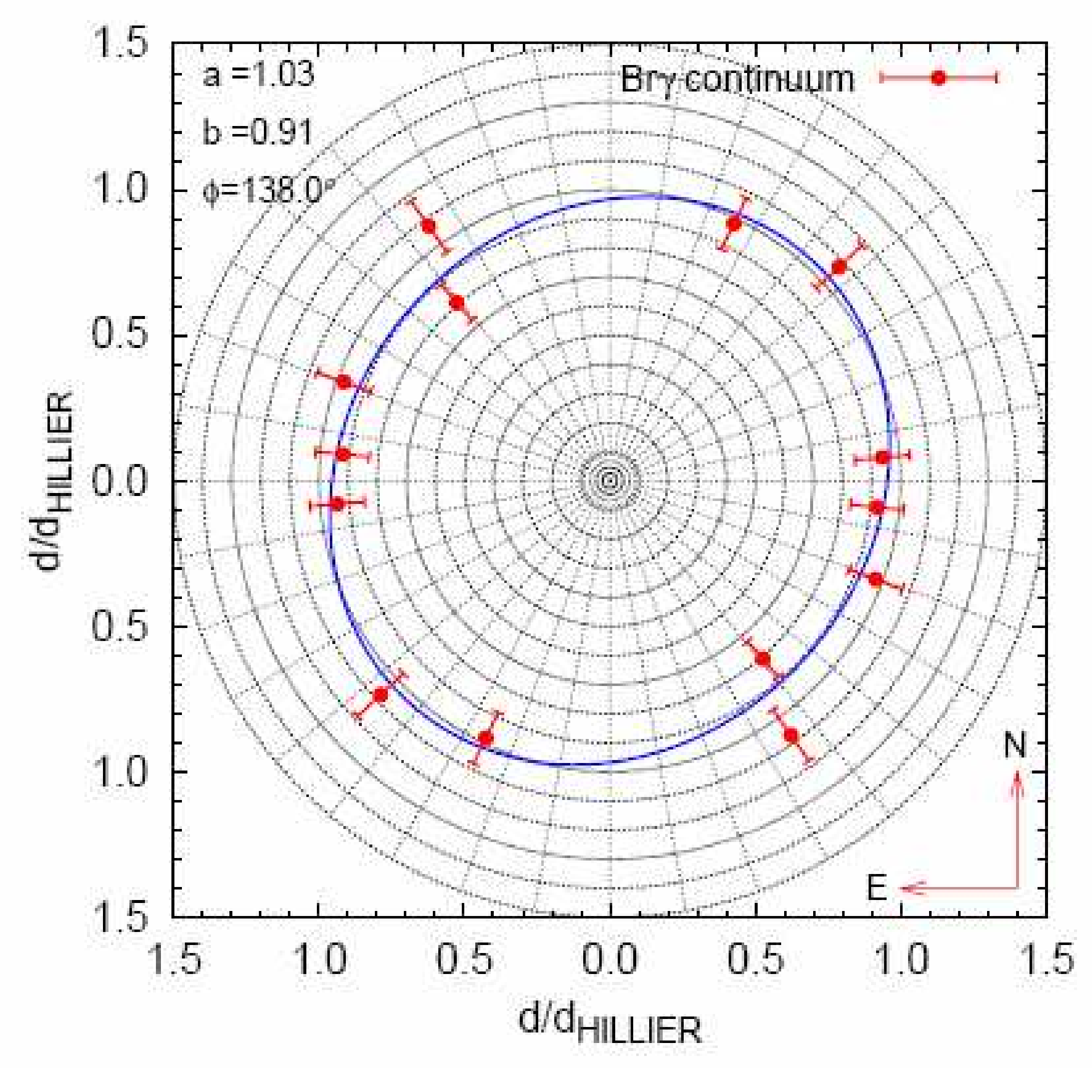

fferential and
ure Phase

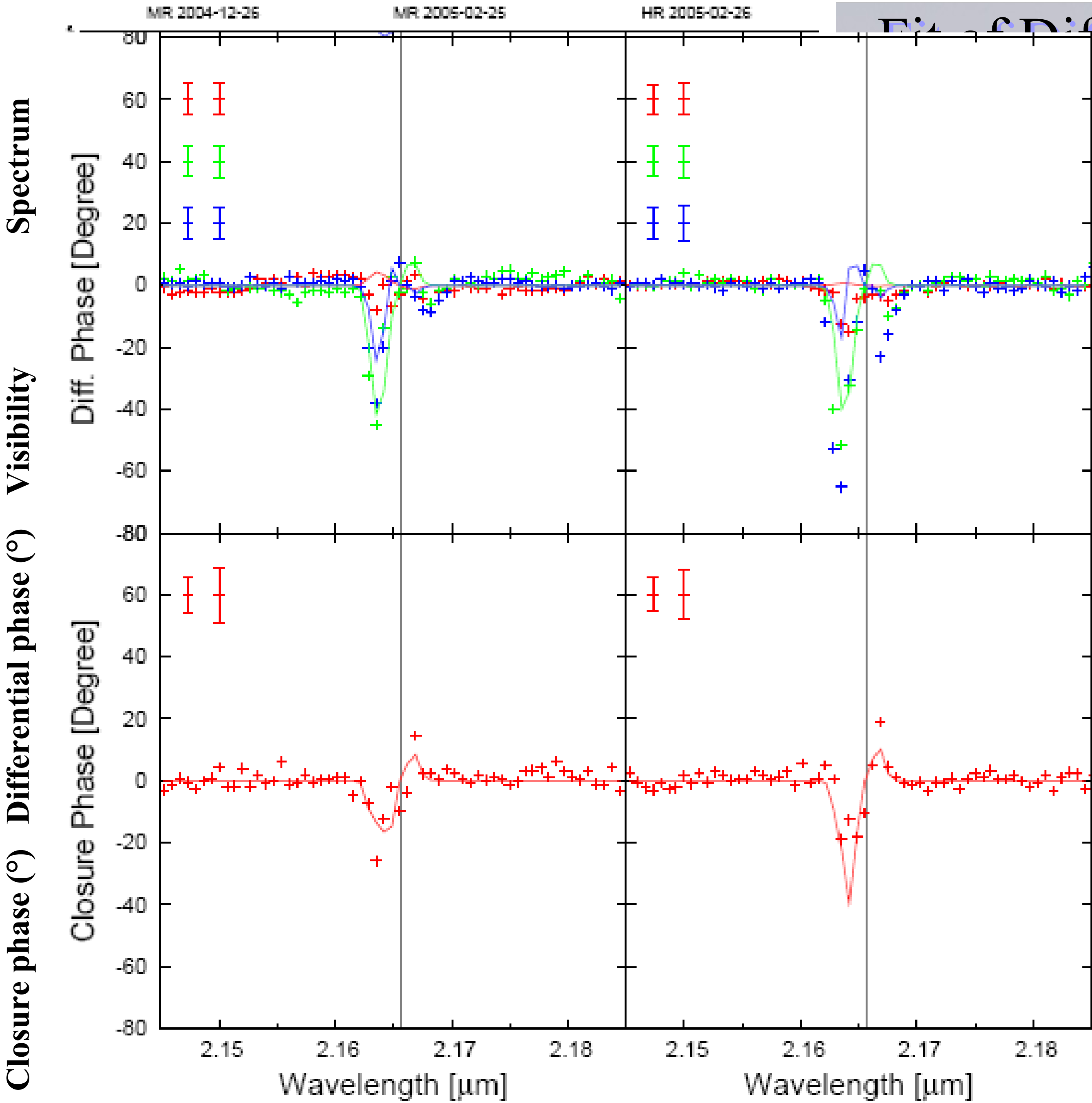

Global « image » of η Car wind

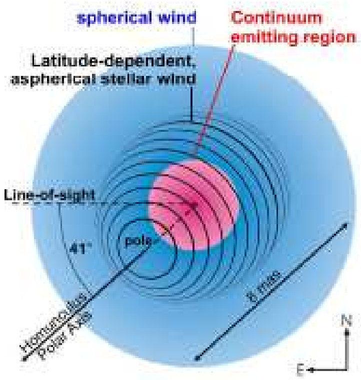

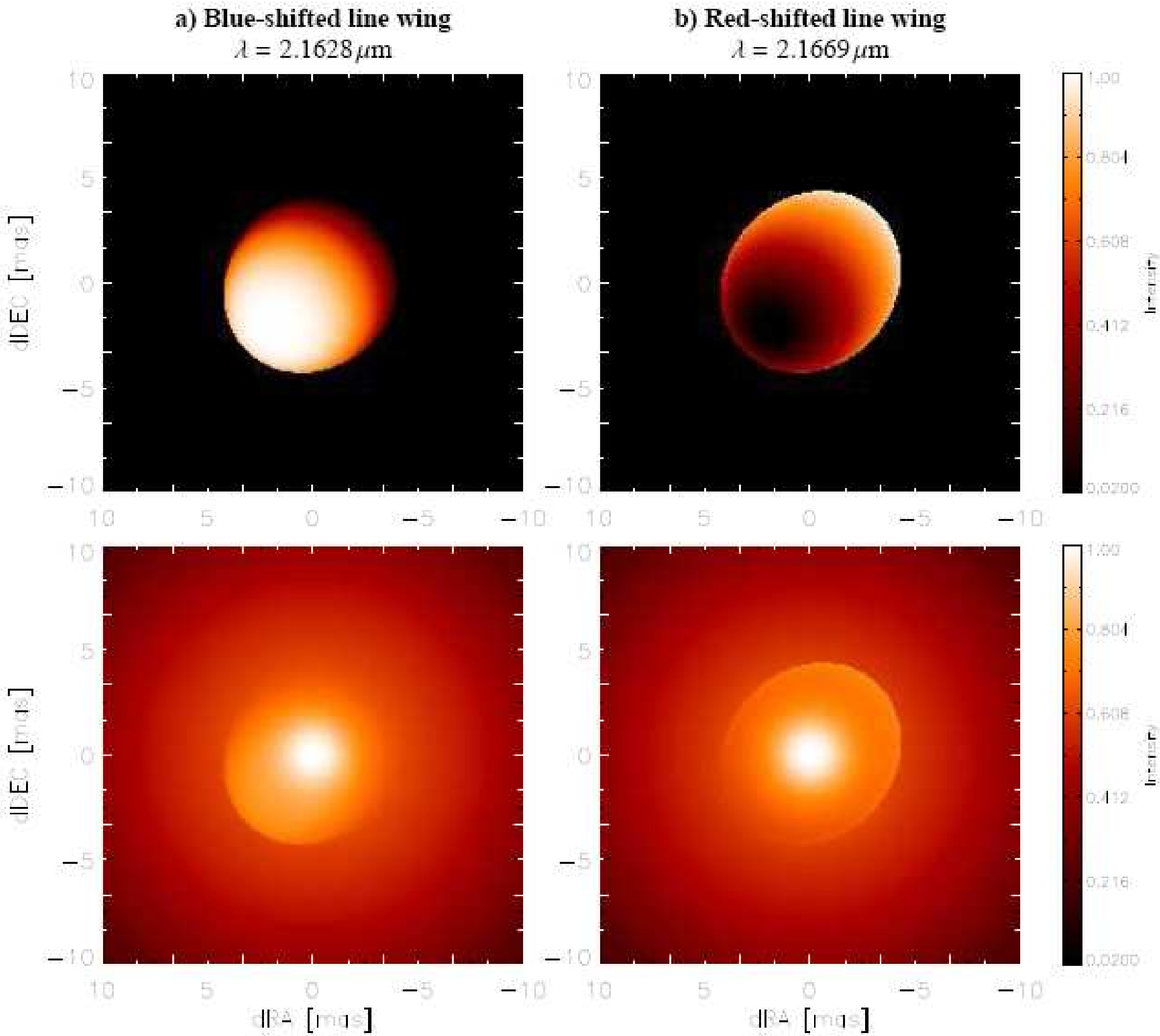

Fig. 10. **Top:** Illustration of the components of our geometric model for an optically thick, latitude-dependent wind (see text for details). For the weak aspherical wind component, we draw the lines of latitudes to illustrate the 3D-orientation of the ellipsoid. **Right (a, b):** The upper row shows the brightness distribution of the modeled aspherical wind component (item (3) in the text) for two representative wavelengths. The figures below show the total brightness distribution after adding the contributions from the two spherical constituents of our model.

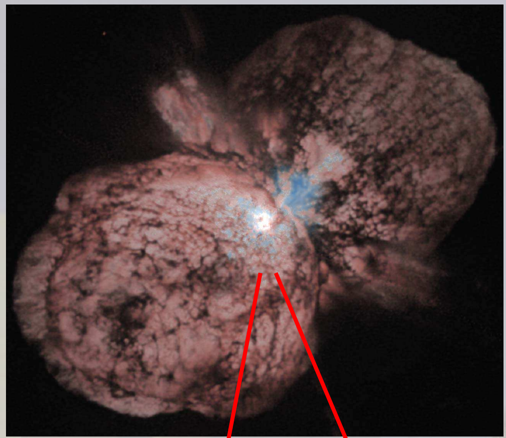

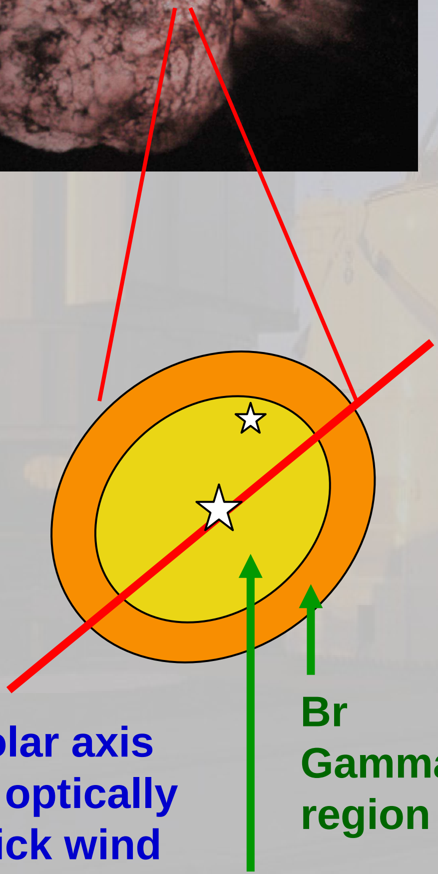

Weigelt et al. 2006 A&A Submitted

Seminar next week

- Resolution of η Car' s optically thick, aspheric wind region
- Wavelength dependence of the visibility
- Good agreement with Hillier et al. 2001 model predictions
- Differential phases and closure phases
- 50% encircled-energy diameter (fit of Hillier et al. model CLVs):

K continuum: 4.3 mas;
Br Gamma: 9.6 mas
He I 2.06 μm: 6.5 mas
elongation with axis ratio 1.21, PA 128°.

- Model can explain the spectrum, all visibilities, differential phases, and closure phases.
- Aspheric wind can be explained by models for line-driven winds from luminous hot stars rotating near their critical speed (Owocki et al. 1996, von Zeipel 1924)

The WR+O binary γ^2 Velorum

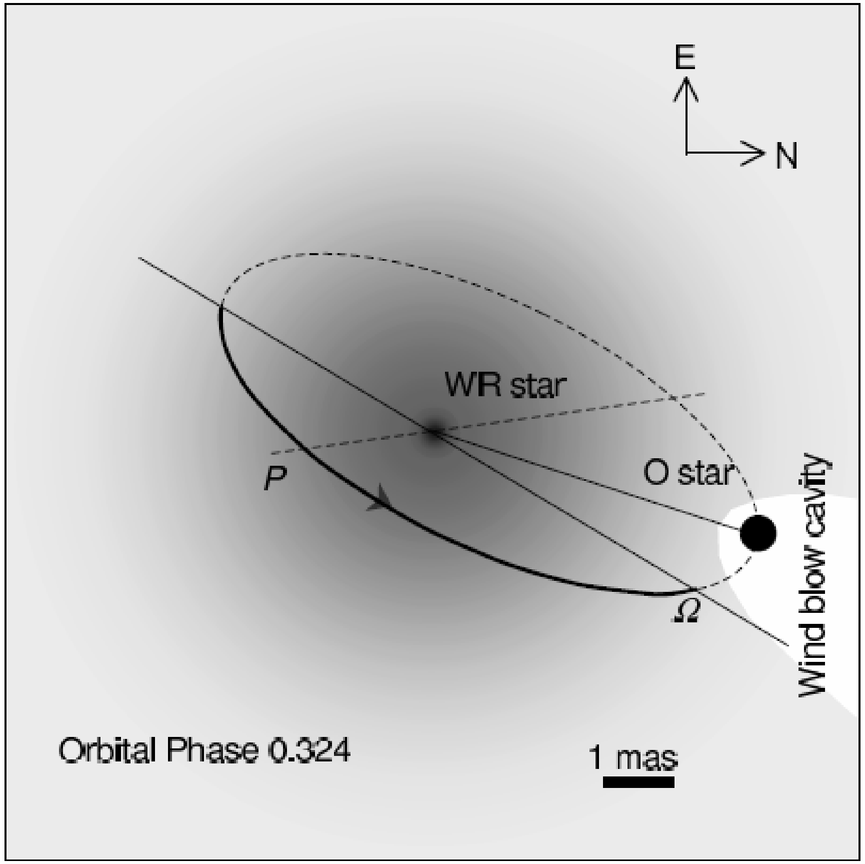

Parameter	Value	Error
Distance	258 pc	+41/-31
Period	78.53 day	0.01
Periastron	2450120.5 day	2
Eccentricity	0.326	0.01
Periastron longitude ω_{WR}	68°	4
a1 sini	39.10^6 km	2.10^6
a2 sini	125.10^6 km	2.10^6
inclination i	63°	3
PA of node Ω	322°	10
R_O	12.4 $R_\odot$	1.7
R_c of WR star	3.0 $R_\odot$	0.5
θ_O	0.48 mas	0.09
θ_c of WR star	0.11 mas	0.06
$\theta_{(\tau_K=1)}$ of WR star	0.28 mas	0.1
$\pi_{(a1+a2)}$	4.8 mas	0.7

Double line spectroscopic binary + « polarimetric orbit » + Intensity Interferometry measure of the separation

Amber measures on γ^2 Velorum

Spectral calibration

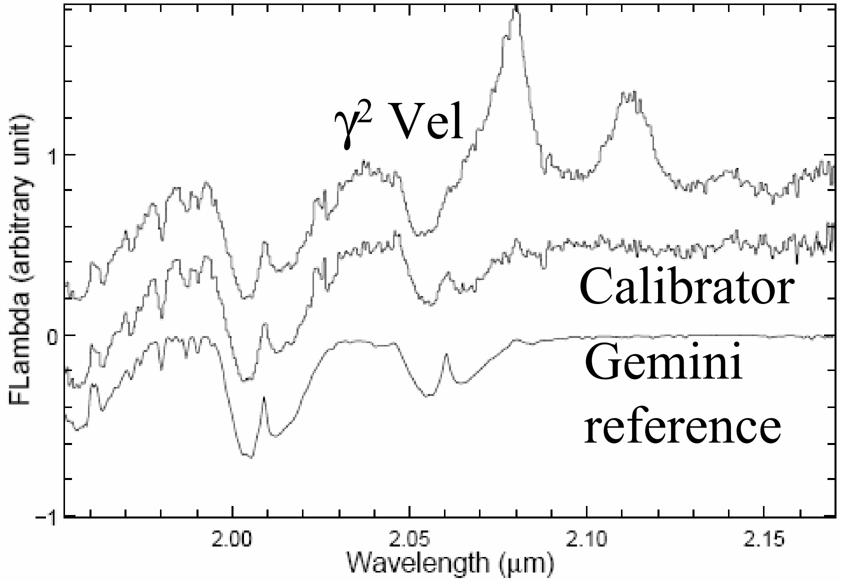

absolute visibility in continuum

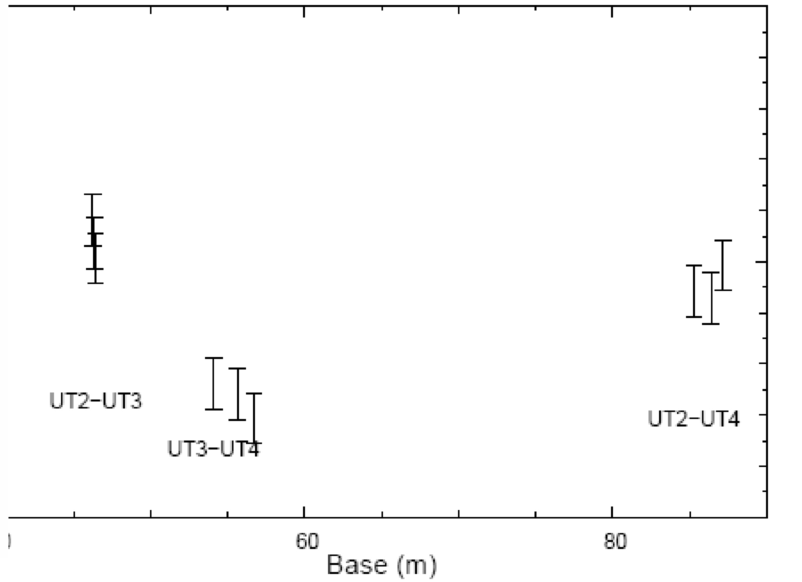

U (m) ------> N

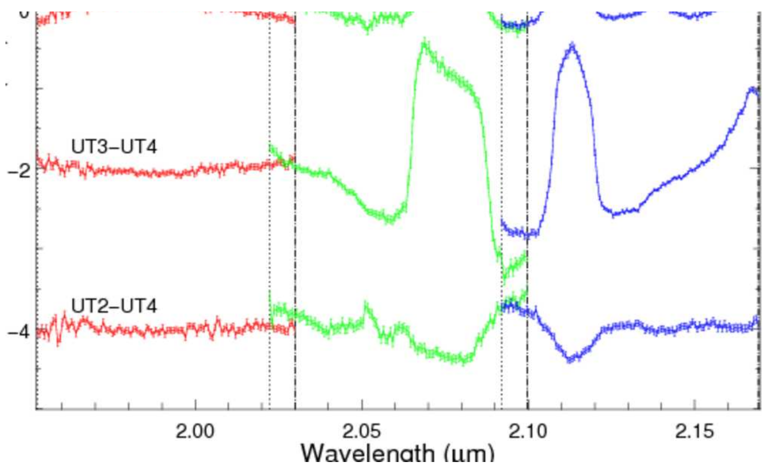

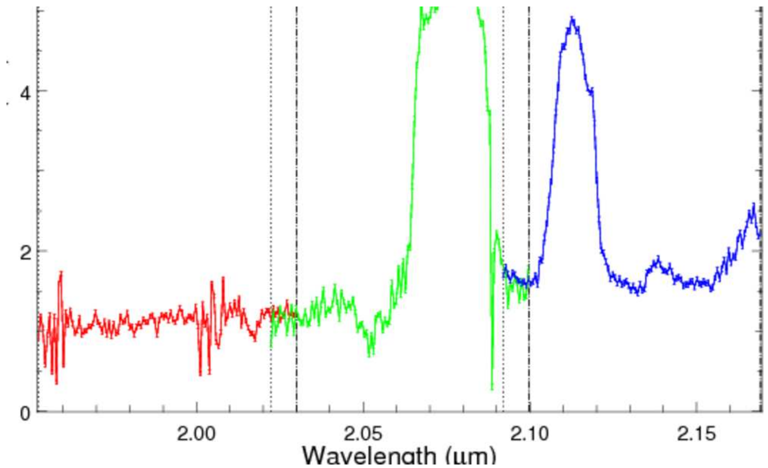

Binary fit from the absolute visibility and the closure phase in the continuum

Wavelength (μm)	1.985	2.025_1	2.025_2	2.045	2.098_1	2.098_2	2.1275	2.150	Avg.	RMS	Δ
					Observation						
Visibility UT2-UT3	0.50	0.52	0.47	0.54	0.54	0.58	0.59	0.59			
Visibility UT3-UT4	0.26	0.26	0.28	0.28	0.23	0.20	0.24	0.26			
Visibility UT2-UT4	0.44	0.43	0.42	0.42	0.41	0.53	0.52	0.48			
Closure Phase	1.09	1.22	1.11	1.37	1.49	1.61	1.78	1.60			
					Fit Binary						
Separation (mas)	3.69	3.68	3.57	3.53	3.60	3.72	3.69	3.68	3.65	0.06	0.1
Position Angle (°)	154.0	154.8	183.4	158.8	166.4	162.3	161.1	160.8	162.7	8.7	10
Flux Ratio 2nd star	0.57	0.57	0.57	0.59	0.64	0.68	0.66	0.64	0.62	0.04	0.1

- Stable binary parameters ρ= 3.65±0.12 mas; PA= 163±13°; WR/O=0.79±0.12
- Poor fit of the visibility (2σ)
- Better if we add a contiuum component in the image accounting for 15% of the flux
- Correlated errors due to the calibrator

Fit of differential measures with best component spectra

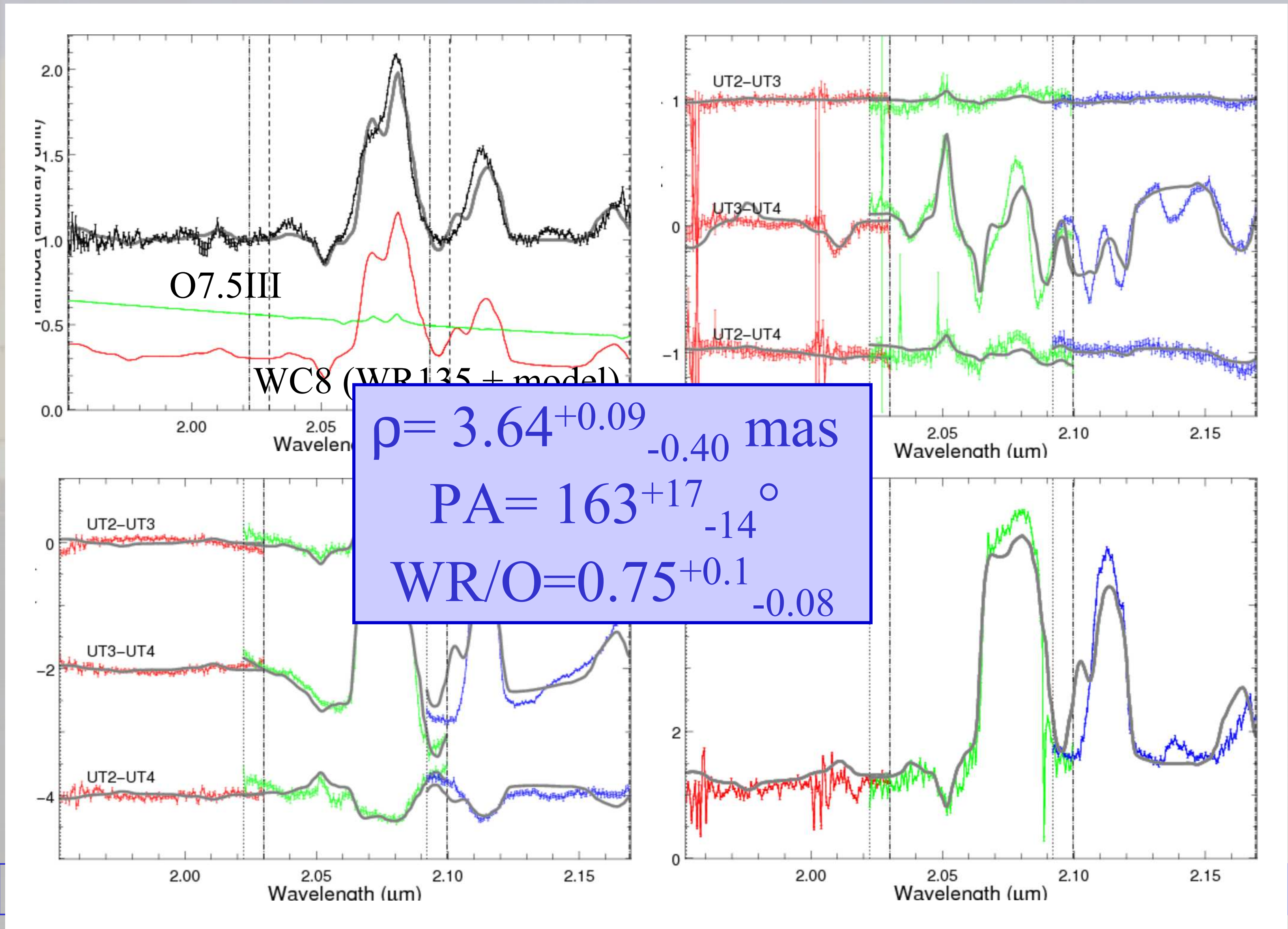

Fit of differential measures with free WR spectrum

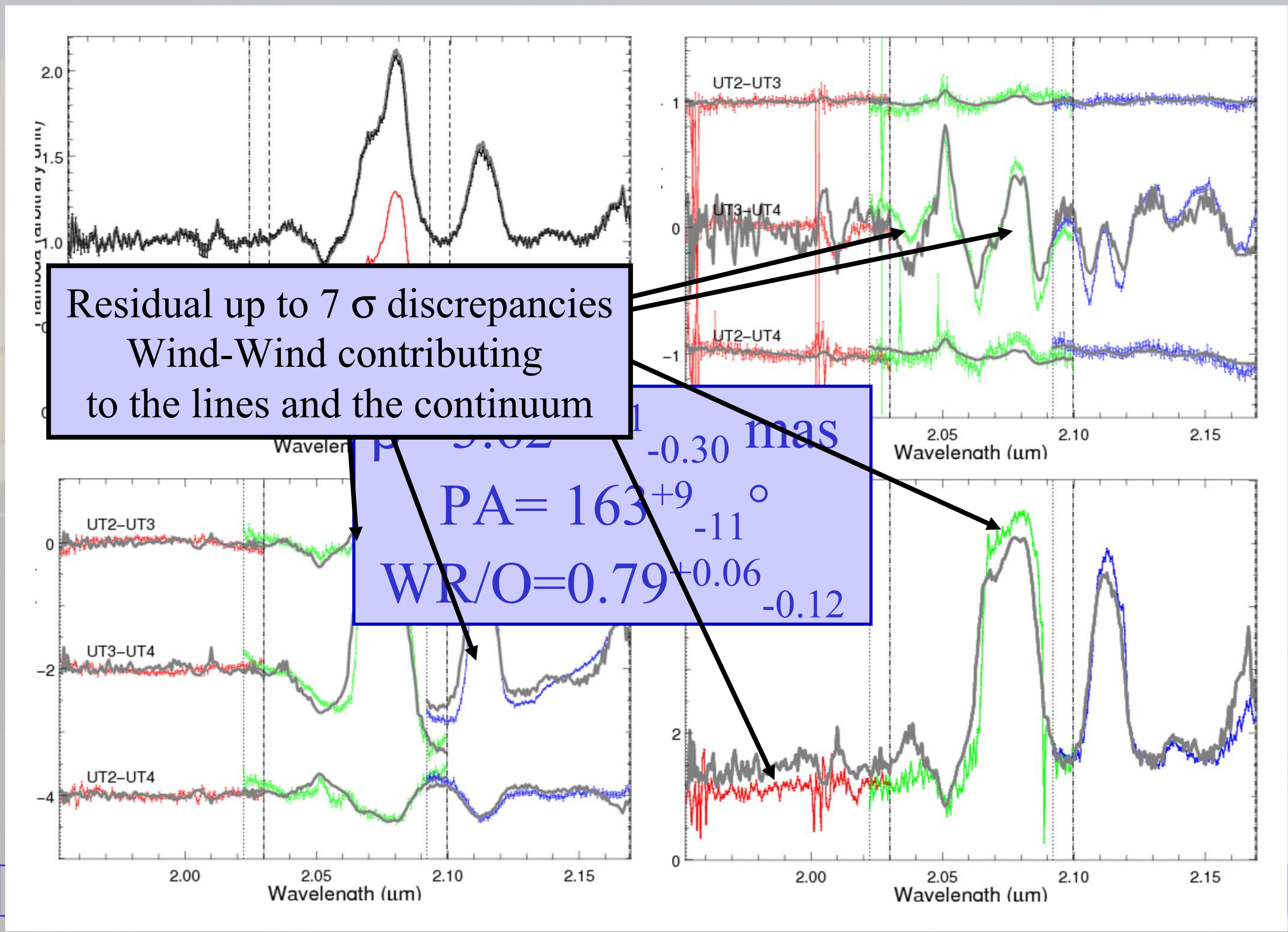

Residual up to 7 σ discrepancies
Wind-Wind contributing
to the lines and the continuum

$_{-0.30}$ mas

PA= 163^{+9}_{-11} °

WR/O=$0.79^{+0.06}_{-0.12}$

The interacting binary γ^2 Velorum

Petrov et al.
2006 A&A
submitted

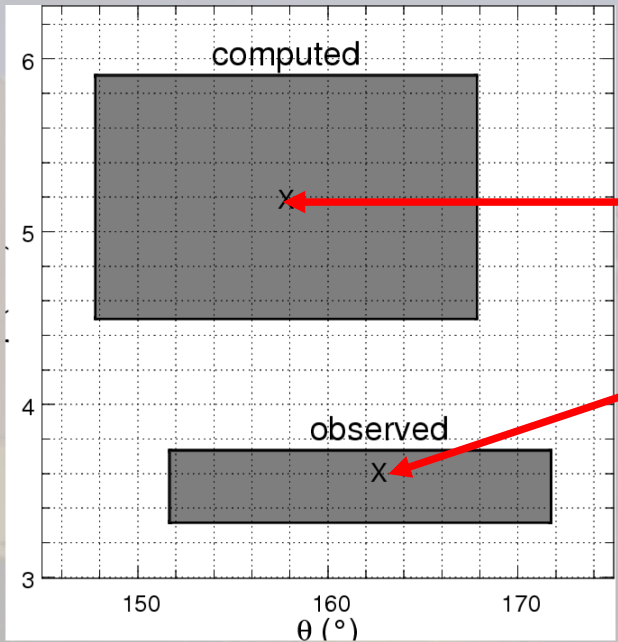

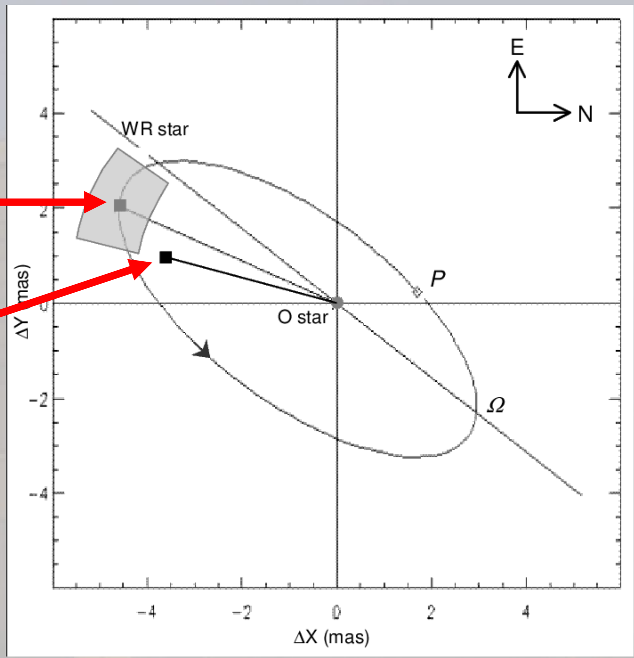

- Binary measurement without a priori knowledge of component spectra
- Reliable binary fit,will not be affected by further fit of continuum or wind-wind
- New computed distance 368 pc
- Detection of the Wind-Wind Collision Zone ?
- Need model of wind-wind line andcontinuum emission or better u-v coverage

Differential phase and extra solar planets

Vannier et al.
2006 MNRAS

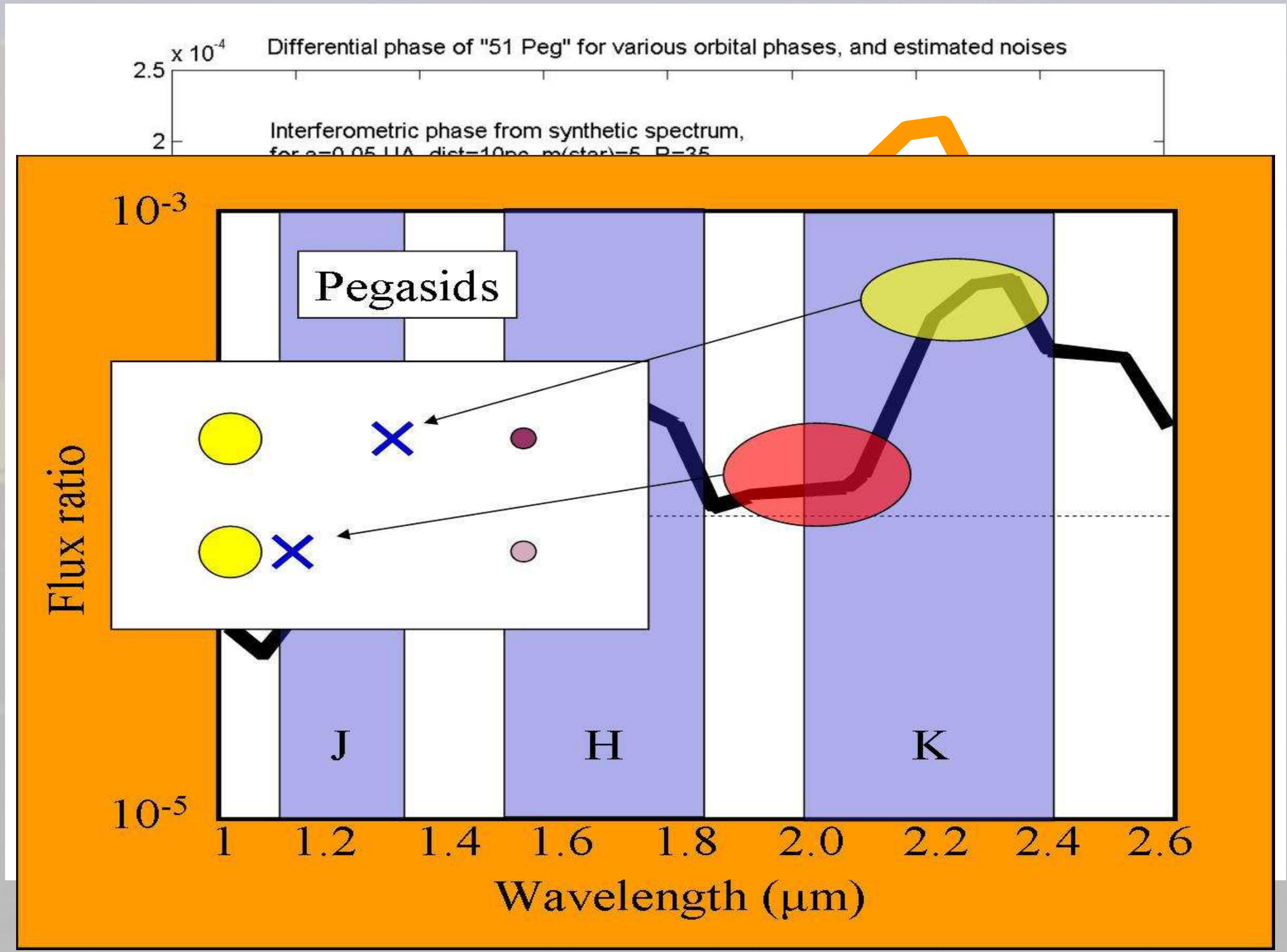

Sources of phase errors

Cause for an error on the differential phase	J		K		Method to eliminate or calibrate
Calibtration cycle	60 s	600 s	60 s	600 s	
Fondamental noise	7.5	2.4	3.9	1.2	Units : 10^{-4} radians.
Atmospheric turbulence	7.2	2.3	1.6	0.5	acceptable
Chromatic dispersion of water vapor (atm+tunnels)	41	13	60	19	Fit (2 parameters) Or Closure phase
Chromatic dispersion of dry air in tunnels	50	17	7	2	
Beam jitter through dichro.	0.7	3.5	0.5	2.5	BCD (60 s) OPD
Beam jitter through polar.	2	10	0.8	4	BCD (60 s) OPD
Beam jitter through ADC	2	3	0	0	BCD (60 s) OPD
Fiber temperature	4	15	2.4	10	BCD (60 s) OPD
Spectrograph deformation	0.08	0.8	0.04	0.4	Negligible
Detector gain changes	4	4	2.6	2.6	BCD (60 s) Non OPD effect
Output beams drift: 1 pixel per week (P2VM change)	10	100	10	100	Non OPD effect Increase beam stability Adapt data processing
Imperfect spatial filtering	?	?	?	>10	Non OPD Introduces a BCD term

Clôture de phase en fonction de λ

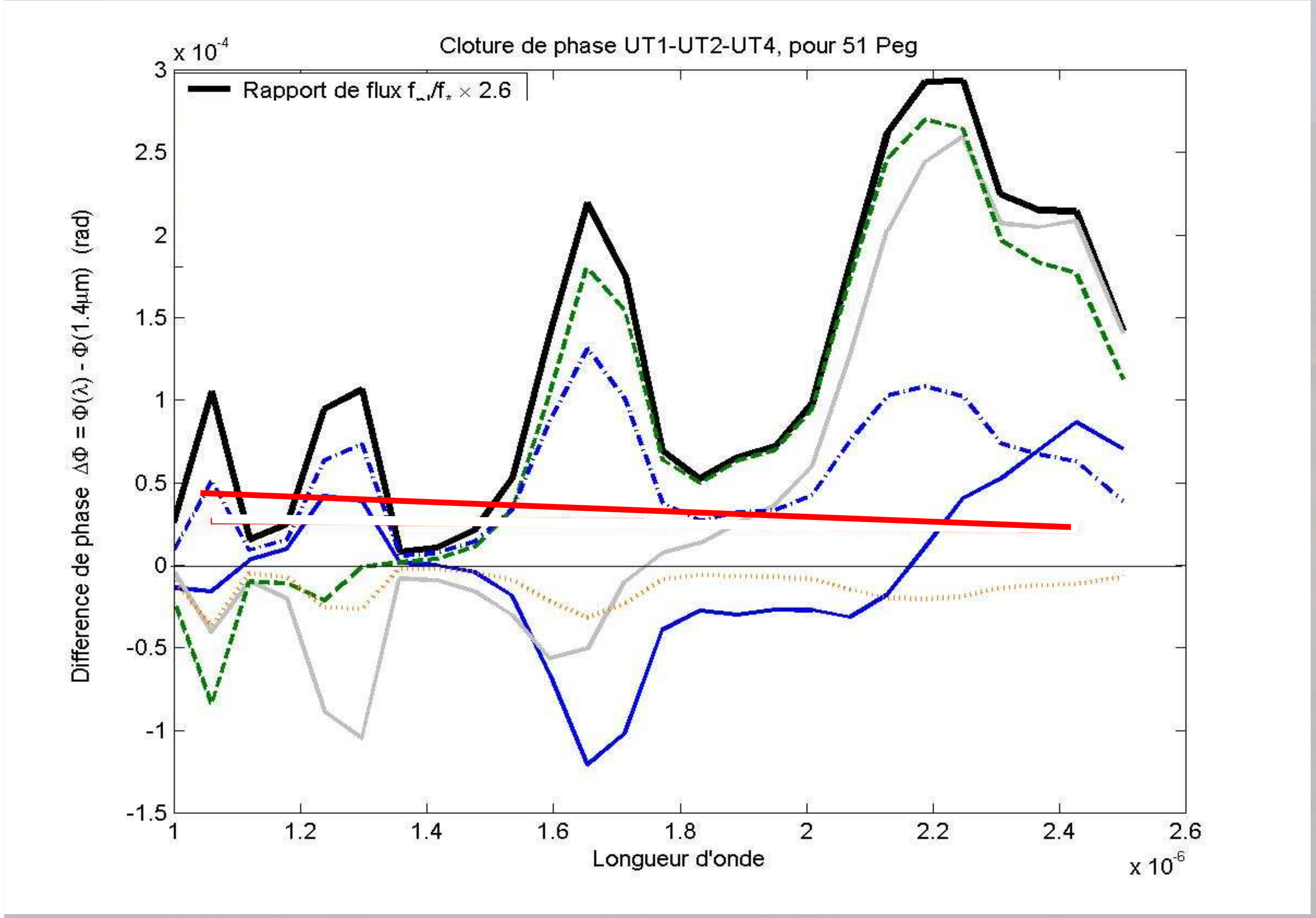

- Phase closure eliminates atmospheric dispersion effects
- It does not eliminate detector effects
- It has a SNR cost:
  - 4.5 more time
  - 6.75 more UT nights

Does phase closure
+ beam commutation
« guarantee »
the result ?

Closure phase calibration with the "Beam Commutation Device"

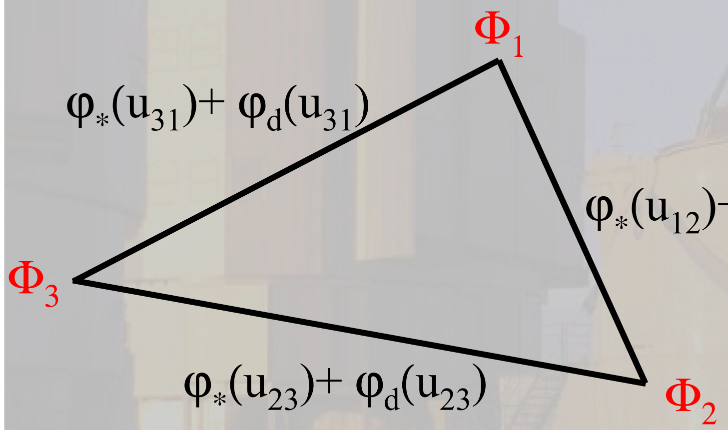

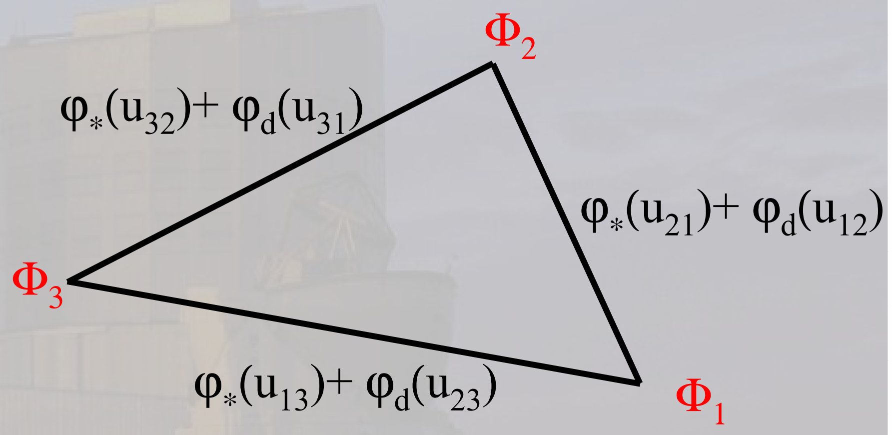

Without BCD:

$\Phi_1 - \Phi_2 + \varphi_*(u_{12}) + \varphi_d(u_{12})$

$\Phi_2 - \Phi_3 + \varphi_*(u_{23}) + \varphi_d(u_{23})$

$\Phi_3 - \Phi_1 + \varphi_*(u_{31}) + \varphi_d(u_{31})$

$-$

With BCD:

$\Phi_2 - \Phi_1 - \varphi_*(u_{12}) + \varphi_d(u_{12})$

$\Phi_1 - \Phi_3 - \varphi_*(u_{31}) + \varphi_d(u_{23})$

$\Phi_3 - \Phi_2 - \varphi_*(u_{23}) + \varphi_d(u_{31})$

$$= 2\,[\varphi_*(u_{12}) + \varphi_*(u_{23}) + \varphi_*(u_{31})]$$

High precision phases: were do we stand ?

- Differential phase below 10^{-3} radians but affected by $n10^{-2}$ radians chromatic OPD:
  - Attempts to fit the chromatic OPD under way
- Closure phase limited to 10^{-2} radians by photon noise and image selection effects. Systematics not met yet.
  - Crucial to stabilize VLTI so we have fringes in all baselines in all frames and therefore good closure phase
  - Use the Ats as soon as 3 Ats are available
- Attempts to use the closure of differential phases

Next targets…

Stellar physics
- Mira, AGB, post-AGB stars
- Young, main-sequence, evolved stars
- Fundamntal stellar parameters (mass, diameter, T_{eff}, age, rotation, distance…)
- Stellar activity (spots and astroseismology)
  - All spectral resolutions for K up to 9 (Finito)

Exoplanet detection
  - Gain a factor 10 to 100 on closure or fit dispersion in differential phase

AGN observation
- Torii, jets, BLR, distances
  - Push VLTI coherent magnitude from 8+ to 11+

Model fitting through all wavelengths
- Discuss regularization function in λ space

Conclusion

Stellar wind structure and kinematics and interaction with the dust (usually concentrated in a) disk

Amber has dramatically increased the number of measures *per baseline*

Strong constraints on morphology and models in spite of very poor u-v coverage for each object

Ubiquity of the equatorial thin disk (dust and/or gas) + latitude dependant wind model

- Selection effect, team bias or breakthrough ?

For most objects observed so far the next step should be:

- 3T observations with a better spectral resolution and/or coverage
- Before a dramatic increase in u-v coverage

The exact potential and limits of spectrally resolved data for model fitting still has to be assessed

Extra Slides

Output pupils

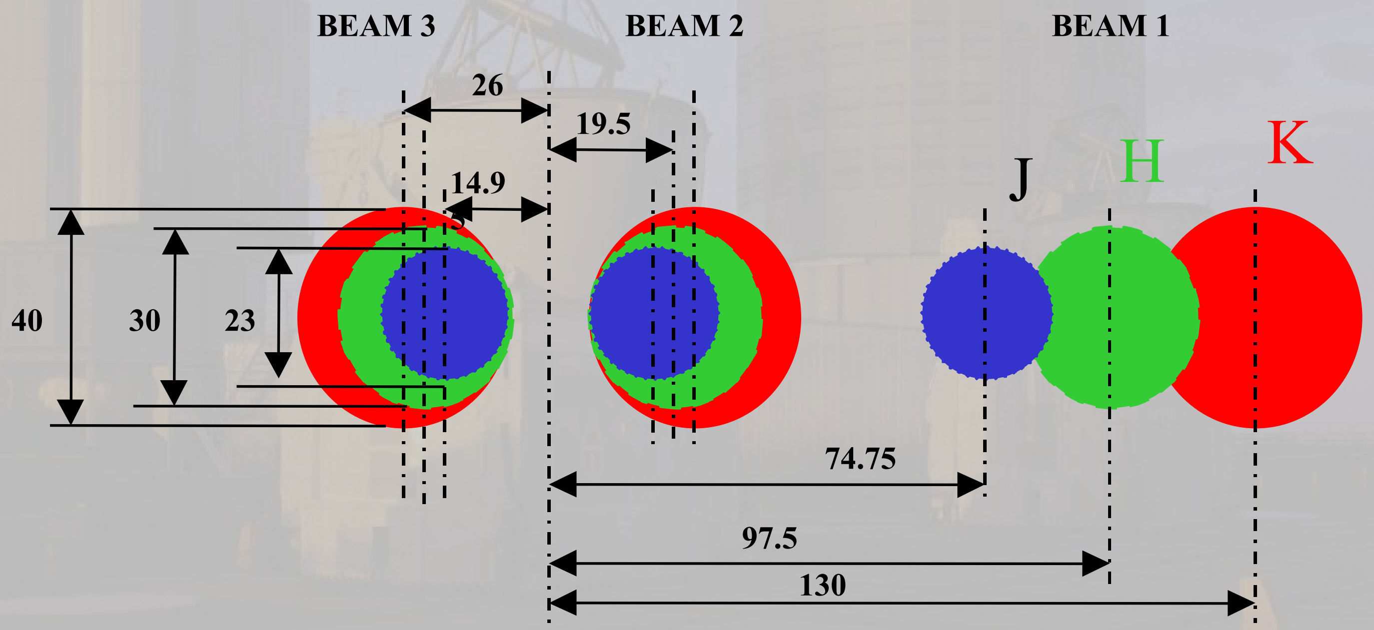

Output Pupils diameters and distances:
the fringe size is the same in the middle of each band.

Differential phase calibration using a "spatial modulation" with a "Beam Commuting Device"

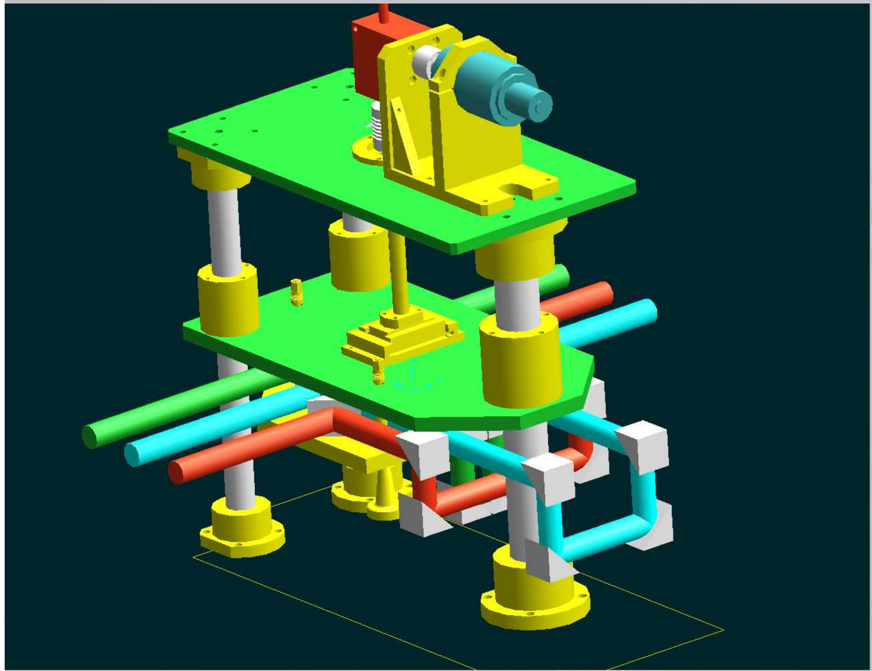

Beam Commuting Device (BCD).
It commutes two of the beams without image inversion. It is activated by inserting the central plate in the beams. It allows to reduce the calibration period down to 60 s or less. To avoid introducing extra effects the specifications are:

- tip-tilt accuracy: 2 arc seconds
- beam jitter accuracy: 10µm
- pupil motion: <30 cm
- opd accuracy: 1 µm

Without BCD:

$$\Delta\Phi_m(\lambda,t_1) = \Delta\Phi_*(\lambda,t_1) + \Delta\Phi_a(\lambda,t_1) + \Delta\Phi_i(\lambda,t_1) + \delta_\Phi(\lambda,t_1)$$

With BCD:

$$\Delta\Phi_{\underline{m}}(\lambda,t_2) = -\Delta\Phi_*(\lambda,t_2) - \Delta\Phi_a(\lambda,t_2) + \Delta\Phi_i(\lambda,t_2) + \delta_\Phi(\lambda,t_2) + \Delta\Phi_{BCD}(\lambda,t_2)$$

Difference:

$$\Delta\Phi_m(\lambda,t_1) - \Delta\Phi_{\underline{m}}(\lambda,t_2) = 2\Delta\Phi_*(\lambda) + 2\Delta\Phi_a(\lambda) + \delta_\Phi(\lambda,t_1) - \delta_\Phi(\lambda,t_2) + \Delta\Phi_{BCD}(\lambda,t_2)$$

The HAe star HD 104237

Herbig A2 star, T_{eff}=8500 K, $L_*=35L_\odot$, $M_*=2.5M_\odot$, D=115 pc

Pole on (i=18°, v sin$i$=12km/s, ring disk with puffed up inner rim at dust sublimation radius…

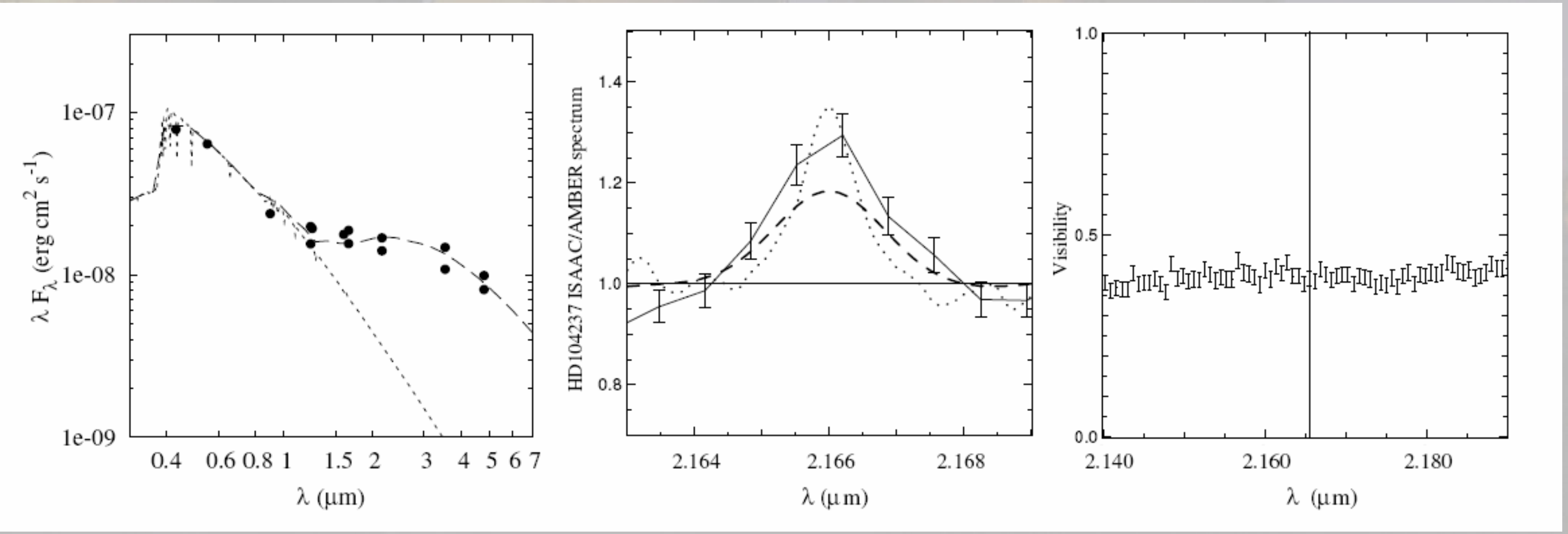

Origin of the wind in HD 104237

Magnetospheric accretion

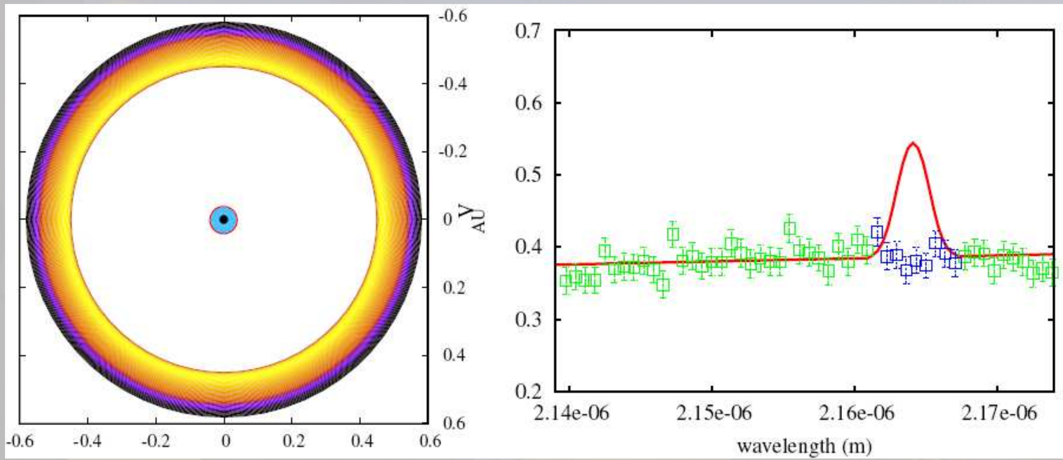

Outflowing wind

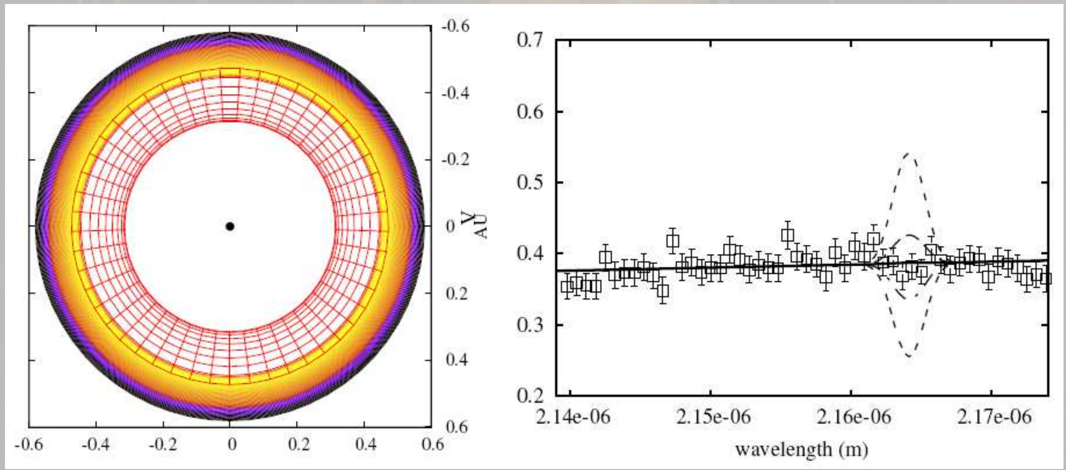

The Gas and the disk regions have an identical equivalent size

Magnetospheric accretion scenario (gas within corotation or magnetoshere radius) is incompatible with AMBER results

Gas filling the disk hole does not work either.

Wind scenario is OK with emission region confined to 0.3-0.5 AU

Which types of wind (stellar, disk or X wind)?

Detection d’ une asymétrie dans le disque de KCMa

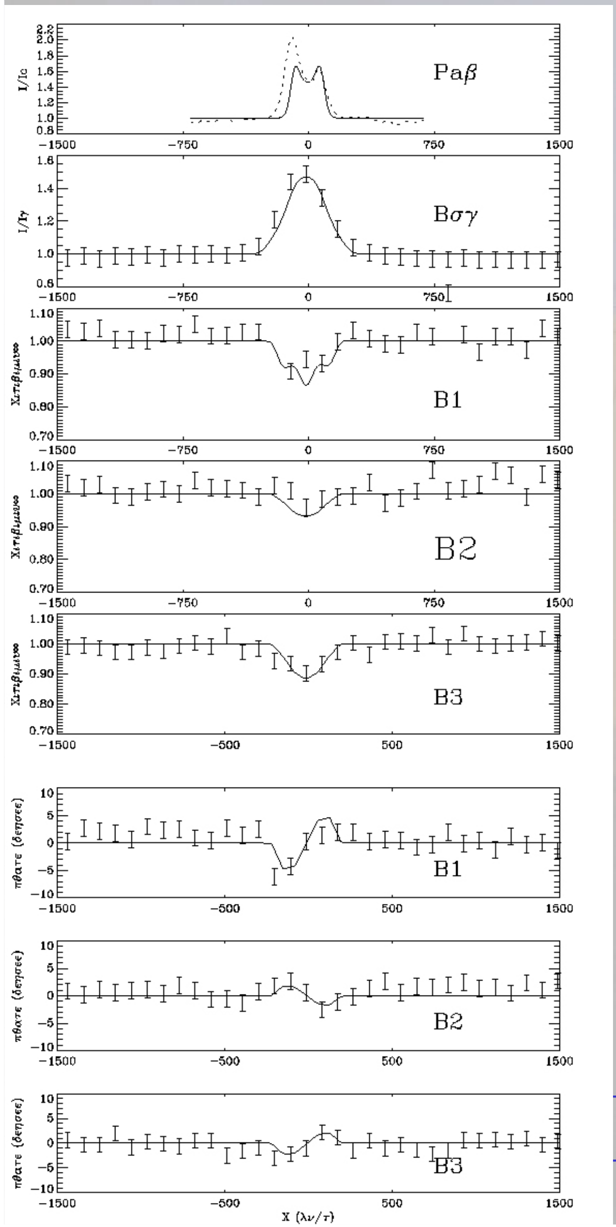

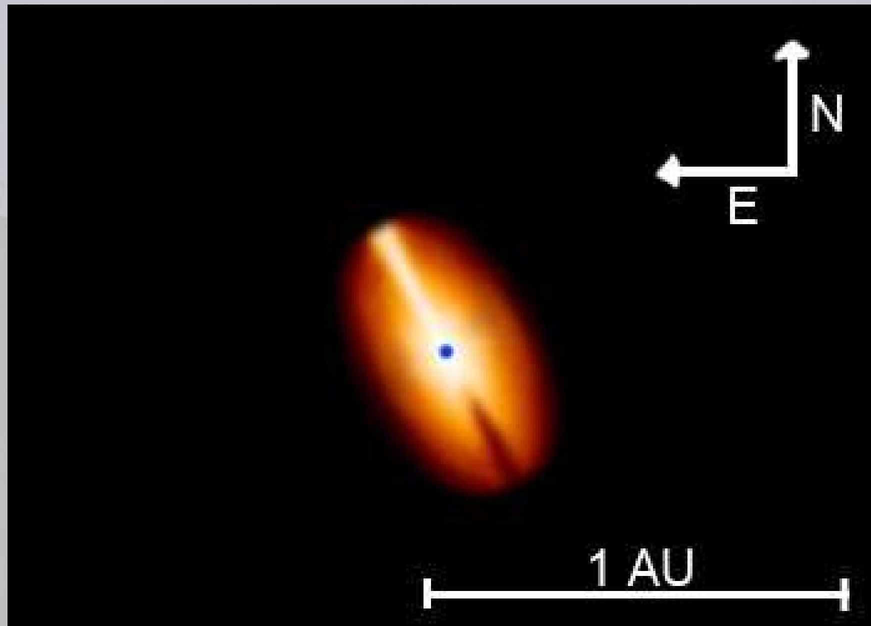

“An asymmetry detected in the disk of KCMa with the VLTI/AMBER” Meilland, A., Millour, F. et al. Submitted to A&A.

B[e] supergiant star CPD-57° 2874

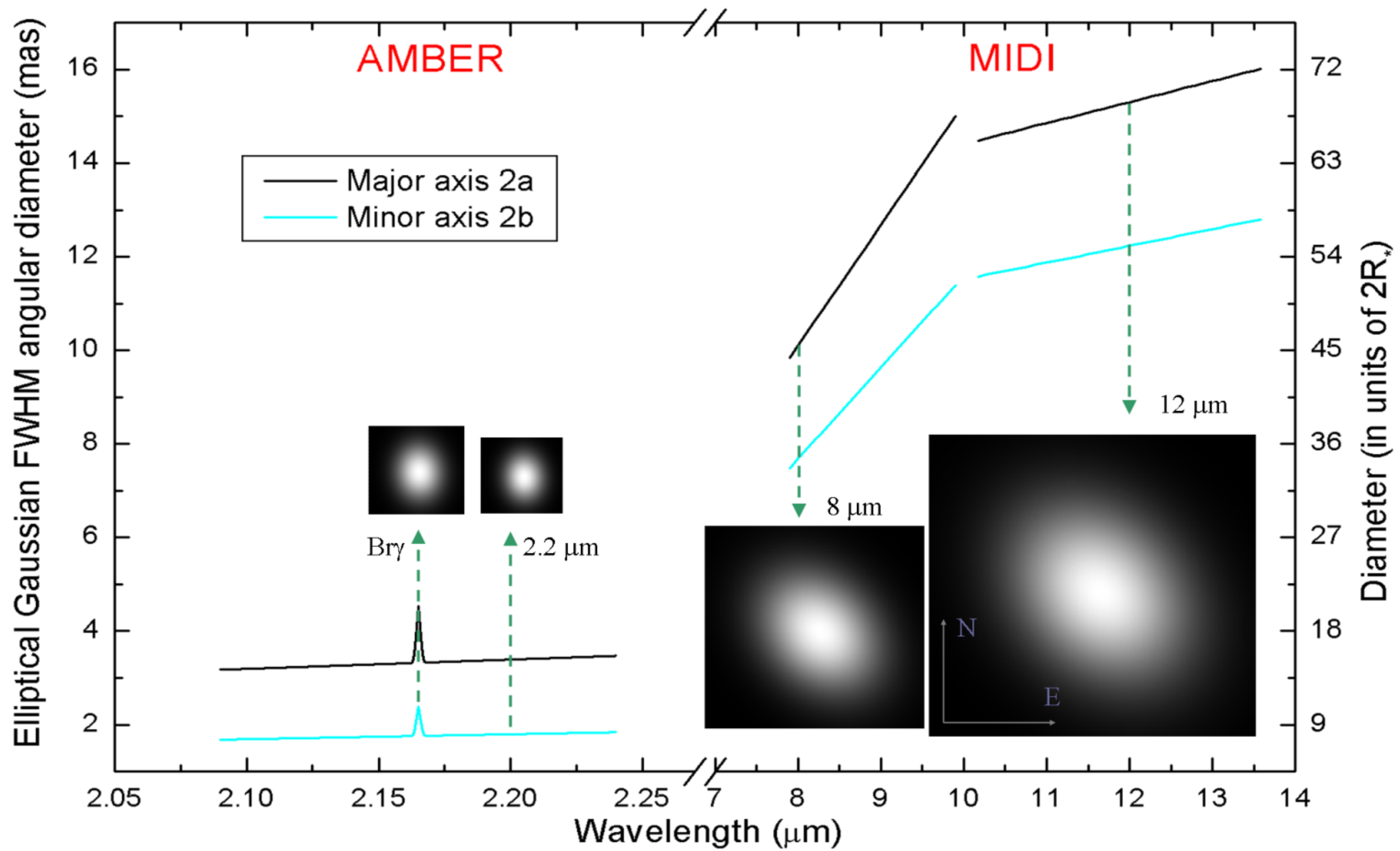

Domiciano de Souza et al. 2006 A&A (astro-ph/0510735)

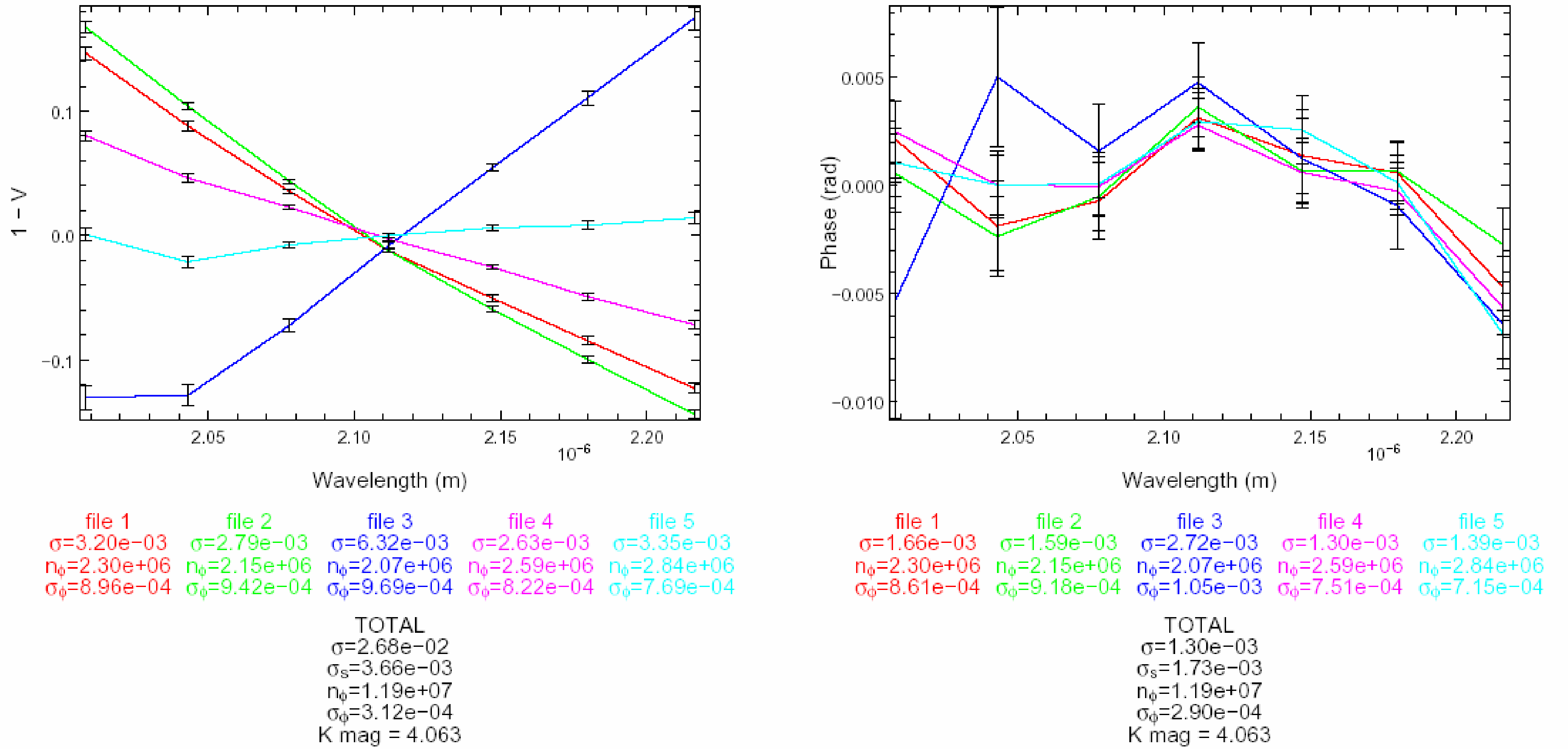

Figure 2. Differential Visibilities and Phases of the calibrator star HD70060.